Postprint of: Szeląg B., Suligowski R., Drewnowski J., De Paola F., Fernandez-Morales F., Bąk Ł., Simulation of the number of storm overflows considering changes in precipitation dynamics and the urbanisation of the catchment area: a probabilistic approach, JOURNAL OF HYDROLOGY, Vol. 598 (2021), 126275, DOI: 10.1016/j.jhydrol.2021.126275

Simulation of the number of storm overflows considering changes in precipitation dynamics and the urbanisation of the catchment area: a probabilistic approach

Bartosz Szeląg[a], Roman Suligowski[b], Jakub Drewnowski[c], Francesco De Paola[d], Francisco J. Fernandez-Morales[e*], Łukasz Bąk[a]

[a] Department of Geotechnics and Water Engineering, Kielce University of Technology, 25-314 Kielce, Poland

[b] Department of Environmental Research and Geo-Information, Jan Kochanowski University, 25-406 Kielce, Poland

[c] Department of Environmental Engineering, Technical University of Gdańsk, ul. Narutowicza 11/12, 80-952, Gdańsk, Poland

[d] Department of Civil, Architectural and Environmental Engineering, University of Naples Federico II, via Claudio 21, Naples 80125, Italy

[e] Chemical Engineering Department, ITQUIMA, University of Castilla-La Mancha, Avenida Camilo José Cela S/N. 13071 Ciudad Real, Spain.

* Corresponding author: Francisco Jesús Fernández Morales

University of Castilla-La Mancha, ITQUIMA, Chemical Engineering Dept., Avda. Camilo José Cela S/N 13071, Ciudad Real, Spain.

Tel: 0034 926 295300 (ext. 6350).

E-mail: fcojesus.fmorales@uclm.es

ORCID: 0000-0003-0389-6247

Abstract

This paper presents a probabilistic methodology that allows the study of the interactions between changes in rainfall dynamics and impervious areas in urban catchment on a long- and short-term basis. The proposed probabilistic model predict future storm overflows while taking into account the dynamics of changes in impervious areas and rainfall. In this model, a logistic regression method was used to simulate overflow resulting from precipitation events based on average rainfall intensity and impervious area. The adopted approach is universal (as it can be used in other urban catchments) and is a significant simplification of classic solutions; a hydrodynamic model is used to analyse the operation of the overflow. For the rainfall simulations, a rainfall generator based on the Monte Carlo method was used. In this method, a modification that allows the simulation of changes taking place in rainfall dynamics, including the effects of climate change, was introduced. This method provides the opportunity to expand and modify probabilistic models in which outflow from the catchment is modelled to predict the functioning of reservoirs and to design sewer networks that have the ability to deal with future rainfall dynamics, including moderate, strong, and violent downpours according to the Sumner scale.

To verify the simulation results with a probabilistic model, an innovative concept using a hydrodynamic model was considered. This verification considers the changes in the impervious area in the period covered by the simulations and is limited using standard calculation procedures.

In practice, the model presented in this work creates opportunities for defining the concept of sustainable development in urban catchments while taking into account the factors mentioned above. From the perspective of landscaping, this is important because it creates the opportunity to limit the impacts of climate change and area urbanization on the receiving waters.

Keywords: logistic regression, storm overflow, probabilistic model, urbanization, rainfall dynamics, sustainability.

1. Introduction

Storm overflows constitute important objects in sewage networks. Based on the main conditions of overflows, including the discharge volume, maximum flow, pollution load and the yearly number of storm overflows, it can be determined whether a studied sewage system operates correctly or requires modernization (Fortier and Malhot, 2015; Tavakol-Davani et al., 2016; Jean et al., 2018). In this case, it is necessary to compare the resulting (determined by measurements) number of storm overflows with their number specified in legal acts and industrial documents. The precise determination of the number of storm overflows and their variation serves an important function since it can be one of the factors upon which the selection of an optimal pattern for the modernisation of a sewage network is based (DWA-M 180E). In numerous cases, modernisation of stormwater management systems is associated with high expenses. It is therefore necessary to optimise the selection of adopted solutions that are already at the design stage of sewage network conversions to achieve the pursued ecological effect (McGrane, 2016; Liu et al., 2017; Zhang et al., 2018).

Assessments of the impacts of adopted sewage network solutions on changes in the number of overflows and the operating conditions of storm overflows are performed using hydrodynamic models (Kleidorfer et al., 2009; McGrane, 2016). Models constitute a useful tool when analysing the operations of sewage networks, but their construction requires a database containing the characteristics of the catchment area and the drainage network as well as measurements of precipitation and flows (with a high temporal resolution). Despite this, these models have a local nature; the cost of their preparation is high, and the results of model simulations do not always correspond to measured data (Elliott and Trowsdale, 2007; Thorndahl and Willems, 2008; Jean et al., 2019). However, access to universal tools that can be used for urban catchment areas with diverse physical-geographical characteristics without the need for model calibration is currently limited. This represents a current problem since

there is a high demand for tools that enable quick analyses of the actions of stormwater drainage systems during the concept formulation stage spatial development in urban areas. Because of this, attempts have been made to construct models that simulate the operations of sewage networks (storm overflows and sewer overflows) and could be used for various catchment areas. Such analyses are presented by Szeląg et al. (2018), who suggest a universal model for simulating the operations of storm overflows. However, these results have not been confirmed by the performance of continuous simulations. Interesting analyses were presented by Thorndahl and Willems (2008) and Grum and Aalderink (1999), who developed empirical models for predicting storm overflow, along with Espino et al. (2018), who presented the possibility of applying logistic regression to sewer overflow simulations. Nonetheless, the determined relationships presented by these and other researchers (Kleidorfer et al., 2009; Gironás et al., 2010; Fu and Kapelan, 2013) had local nature; therefore, it was not possible to apply them to other catchment areas.

To enable the assessment of storm overflow operations, it is necessary to perform continuous simulations, which require multiannual precipitation data. However, studies performed by numerous teams of scientists indicate that the dynamics of precipitation (frequency, magnitude, intensity) varies as a result of climate change (Wu et al., 2013). This is why, at the stage of sewage network simulations, it seems appropriate to present the impacts of changes in rainfall dynamics on the operations of sewage networks over consecutive years. This is very important, as it allows the optimal selection of a sustainable development concept for a given catchment area (Huong and Pathirana, 2013; Kirshen et al., 2014). However, the construction of a model for simulating rainfall variations caused by climate change is a complicated task that requires the implementation of complex numerical algorithms (Boyle, 1998; Sharma et al., 2007). In engineering considerations, this task is difficult to perform; therefore, the need arises for the development of a simplified methodology. Precipitation data

acquired by means of climatic models (CGM, LGM, etc.) constitute input information necessary for continuous simulations (Gironás et al., 2010; Arnell, 2011; Arnbjerg-Nielsen et al., 2013). The produced results of the simulations are significant from a practical point of view in terms of the modernisation of sewage networks with the consideration of climate change. However, in the abovementioned approach, some authors (Adams and Papa, 2000; Kleidorfer et al., 2009) usually apply limited considerations of changes in impervious areas. Additionally, in numerous analyses, the dynamics of changes in the impervious of a catchment in the long term is considered within a limited scope.

Due to the above, it is appropriate to develop a computational methodology that allows the simultaneous analyses of the impacts of changes in rainfall dynamics (in the long and short term) and the dynamics of urbanisation, and the yielded results should be characterised by strong compliance with theoretical data. In terms of land development plans for cities, it seems desirable to make an attempt aimed at the development of an optimal concept for the urbanisation of catchment areas in a manner in which negative impacts on the receiving waters are as limited as possible while considering the nature of rainfall, i.e., to minimise the number of storm overflows affecting the heavy pollution of receiving waters. This paper presents a concept of the construction of a probabilistic model for simulating the number of storm overflows (in a short- and long-term approach) while not only incorporating the dynamics of changes in rainfall intensity in the consecutive years covered by the simulations but also allowing an analysis of this phenomenon considering the progressing urbanisation of the catchment area. This paper also presents a research methodology allowing optimisation of the concept of sustainable development of a catchment area, involving the limitation of the number of storm overflows and taking into account the variable dynamics of rainfall. This study presents two parallel approaches, i.e., simulation of the number of storm overflows determined by a mathematical model (considering changes in rainfall dynamics in a

multiannual approach and changes in the impervious area of the catchment) and the comparisons among these simulations and calculations using a calibrated hydrodynamic model.

2. Study area

The research area comprises an urban catchment area covering 62 ha located in the south-eastern part of Kielce city (Fig. 1). The city is located in the southern part of Poland and is the capital of Świętokrzyskie Province. It occupies an area of 109 km^2. The average population density is 17.9 people·ha^{-1}. The highest point in the catchment area is at an elevation of 271.20 m a.s.l., and the lowest point is at 260.00 m a.s.l. The average slope of the land in the catchment area is 7.1%. Within the catchment area, there are housing estates, public utility buildings and a network of roads with a density of 108 m·ha^{-1}. Over the last 10 years (2009-2019), there was visible intensification of urbanisation processes in the studied catchment area, which caused an increase in the share of impervious areas (Imp) from 33% to 55% (in the period 2009-2011, the impervious areas changed from Imp = 33% to Imp = 38%, while in 2014 it reached the value of Imp = 41% – Appendix A). The roofs of buildings currently occupy 16.5% of the whole catchment area, and 17.7% of the whole area is covered by roads, 12.2% by parking areas and 8.6% by pavement. The remaining portion of the catchment area (45%) is covered by urban greenery.

This paper analyses a separate storm sewer system. Only treated stormwater is delivered by the S1 storm sewer to the Silnica River. The main canal, with a diameter of ϕ 600-1250 mm, has a length of 1569 m, and its gradient ranges from 0.04% to 3.90%. This sewer collects stormwater from approximately a side sewers (ϕ 300-1000 mm) (Fig. 1), the slope of which do not exceed 2.61%. The total length of the drainage network is 11,375 m. The volume of the sewers and drainage manholes is 2032 m^3. Stormwater from the catchment area is

discharged via the S1 sewer to a stormwater treatment plant (STP) by means of a flow divider (DC). When the level of stormwater in the DC is lower than h_{min} = 0.42 m, their entirety flows to the STP. In contrast, when the level of stormwater exceeds the value of h_{min}, a storm overflow (OV) occurs, and a portion of the stormwater is delivered directly (without treatment) to the the Silnica River.

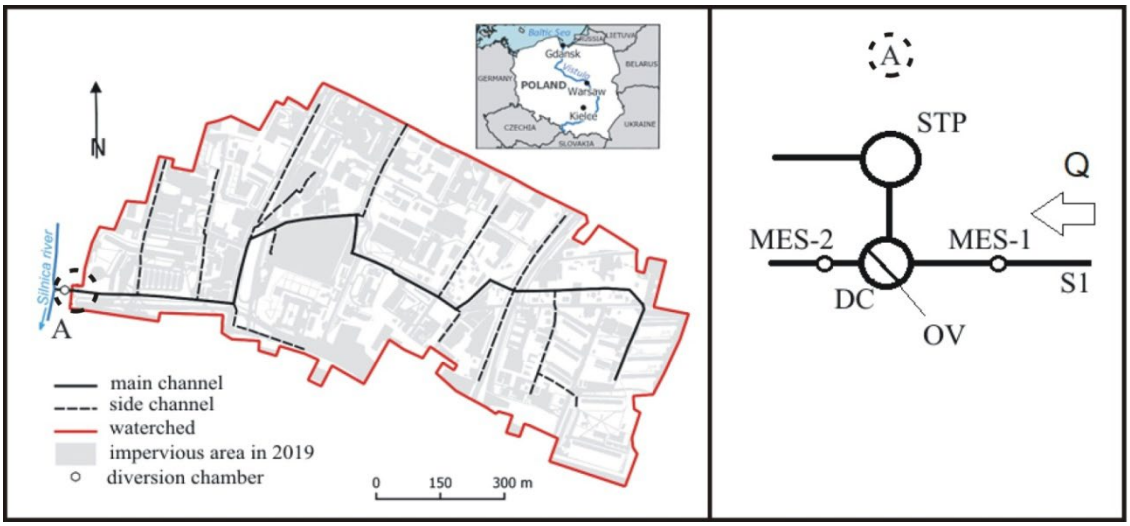

Fig. 1. Study area.

In the analysed urban catchment area, continuous measurements of flows and filling levels were performed in the years 2009-2011 by means of an MES-1 flow metre installed in the S1 sewer at a distance of 3.0 m from the DC. The flow metre measures the flow and filling level with a resolution of 1 minute. The probe of the flow metre measures the level (by measuring the water level pressure) and average flow rate of stormwater (via the Doppler effect), which, with the specific shape and dimensions of the canal, allow the calculation (by means of a built-in microprocessor) of the volumetric flow rate of the stormwater. Moreover, in 2015, another MES-2-type flow metre was installed in the sewer downstream of the storm overflow. An analysis of the collected measurement data (from 2008-2017) demonstrated that the annual rainfall depth varied within a range of 537-757 mm, and the number of rainy days ranged from 155 to 266. The length of the dry period was 0.16-60 days. Moreover, it was

concluded that storms occurred 27-47 times a year. The average annual air temperature in the studied period was 8.1-9.6 °C, and the number of days with snowfall ranged from 36 to 84. At the same time, an analysis of the flow measurement data recorded by means of the MES-1 flow metre demonstrated that the momentary flow rate of stormwater in dry periods ranged from 1 to 9 $L \cdot s^{-1}$, which indicated the occurrence of infiltration in the studied sewer network.

3. Methodology of research

3.1. The model of overflow operations, taking into account climate changes and urbanisation of the catchment area

The impact of the intensity of rainfall and the progressing urbanisation of the catchment area in *t* consecutive years on the occurrence of storm overflows can be described by the following relationships:

$$[P_1, P_2, P_3, \dots, P_i, t_r]_{1,t=1}, [P_1, P_2, P_3, \dots, P_i, t_r]_{2,t=1}, [P_1, P_2, P_3, \dots, P_i, t_r]_{\mathrm{m},t=1}, \dots, [P_1, P_2, P_3, \dots, P_i, t_r]_{\mathrm{j},t=\mathrm{k}} \quad (1)$$

$$[0, Q_1, Q_2, \dots, Q_i]_{1,t=1}, [0, Q_1, Q_2, \dots, Q_i]_{2,t=1}, [0, Q_1, Q_2, \dots, Q_i]_{m,t=1} \dots, [0, Q_1, Q_2, \dots, Q_i]_{\mathrm{j},t=k} \quad (2)$$

$$T = \begin{cases} 0 \text{ when } \mathrm{h}(Q_\mathrm{i})_\mathrm{j} < \mathrm{h_g} \\ 1 \text{ when } \mathrm{h}(Q_\mathrm{i})_\mathrm{j} > \mathrm{h_g} \end{cases} \quad (3)$$

which results in:

$$T_{1,\mathrm{t}=1}, T_{2,\mathrm{t}=1}, T_{3,\mathrm{t}=1}, \dots, T_{\mathrm{j,k}} \quad (4)$$

$$\mathrm{Imp}_1, \mathrm{Imp}_2, \mathrm{Imp}_3, \dots, \mathrm{Imp}_{\mathrm{t=k}} \quad (5)$$

Therefore, every rainfall event that corresponds to an operating overflow state can be described by the following vector:

$$[T]_{\mathrm{j,k}} = [P_1, P_2, P_3, \dots, P_\mathrm{i}, t_\mathrm{r}, \mathrm{Imp_k}] \quad (6)$$

where

P_1, P_2, P_3,…, P_i, t_r – the rainfall characteristics of a single j-th precipitation event (*P* represents rainfall depth or rainfall intensity and t_r represents rainfall duration), Imp – the impervious area of the catchment, j – the number of rainfall events in a year (i = 1, 2,

3,…, j), t – the time period covered by the calculations (t = 1, 2, 3,..., k), h(Q_i)$_j$ – the filling level at the storm overflow, and h_g indicates the height of the edge of the storm overflow.

For a task set in this manner, the storm overflow is interpreted as a binary variable as presented in equation (3). This is why, based on the data, including measurements of precipitation characteristics in independent precipitation events and the operations of the overflow, it is possible to develop a classification model to simulate the operation of the overflow. In a multiannual approach, the impact of climate change and its trend in a time series can be identified in the proposed model based on variations in the values of estimated parameters, θ_n, in theoretical distributions, $f(P_i)$, describing rainfall characteristics in the following form:

$$\theta_n = f(\mathrm{t} = \mathrm{k}) \tag{7}$$

where

f(t) – an empirical model to determine the values of parameters in the theoretical distribution for the consecutive t years covered by the calculations, n – the number of parameters determined in the theoretical distribution.

On this basis, it can be stated that the values of precipitation characteristics in the consecutive t years in a time series are as follows:

$$[P_1, P_2, P_3, \dots, P_i, t_r, \theta_{1,n}]_{1,2,3,\dots,j,t=1}, [P_1, P_2, P_3, \dots, P_i, t_r, \theta_{2,n}]_{1,2,3,\dots,j,t=2}, [P_1, P_2, P_3, \dots, P_i, t_r, \theta_{2,n}]_{1,2,3,\dots,j,t=k} \tag{8}$$

In contrast, the events for which the function of an overflow can be described in a single episode are defined by the relationship:

$$[T]_{j,k} = [P_1, P_2, P_3, \dots, P_i, t_r, \theta_{n,k}, \mathrm{Imp}_k] \tag{9}$$

where

$\theta_{n,t}$ – the numerical values of n parameters in a theoretical distribution, describing precipitation characteristics for the k, z, or t years covered by the calculations.

The relationships presented above constitute a basis for calculating the number of storm overflows in short-term (e.g., a single episode) or long-term approaches (1, 2, or 5 years), which can take into account both changes in the impervious area of the catchment (Imp) and changes in the rainfall dynamics that result from climate changes.

3.2. An algorithm for the construction of a probabilistic model for analysing the operation of a storm overflow

A probabilistic storm overflow model designed to simulate the number of storm overflows in both short- and long-term approaches was developed as part of the performed analyses. In contrast to the models developed by other researchers (Fortier and Maihot, 2015; Jean et al., 2018), the suggested approach will take into account the dynamics of urbanisation processes and changes in precipitation at the same time. Therefore, the suggested solution enables an analysis of the interaction between an increase in rainfall intensity and an increase in the impervious area of the catchment in a multiannual approach. The developed methodology also enables an assessment of the impacts of the uncertainty associated with the identification of rainfall dynamics in short- and long-term approaches on storm overflow operations. The computational algorithm used to construct a probabilistic model is presented in Fig. 2.

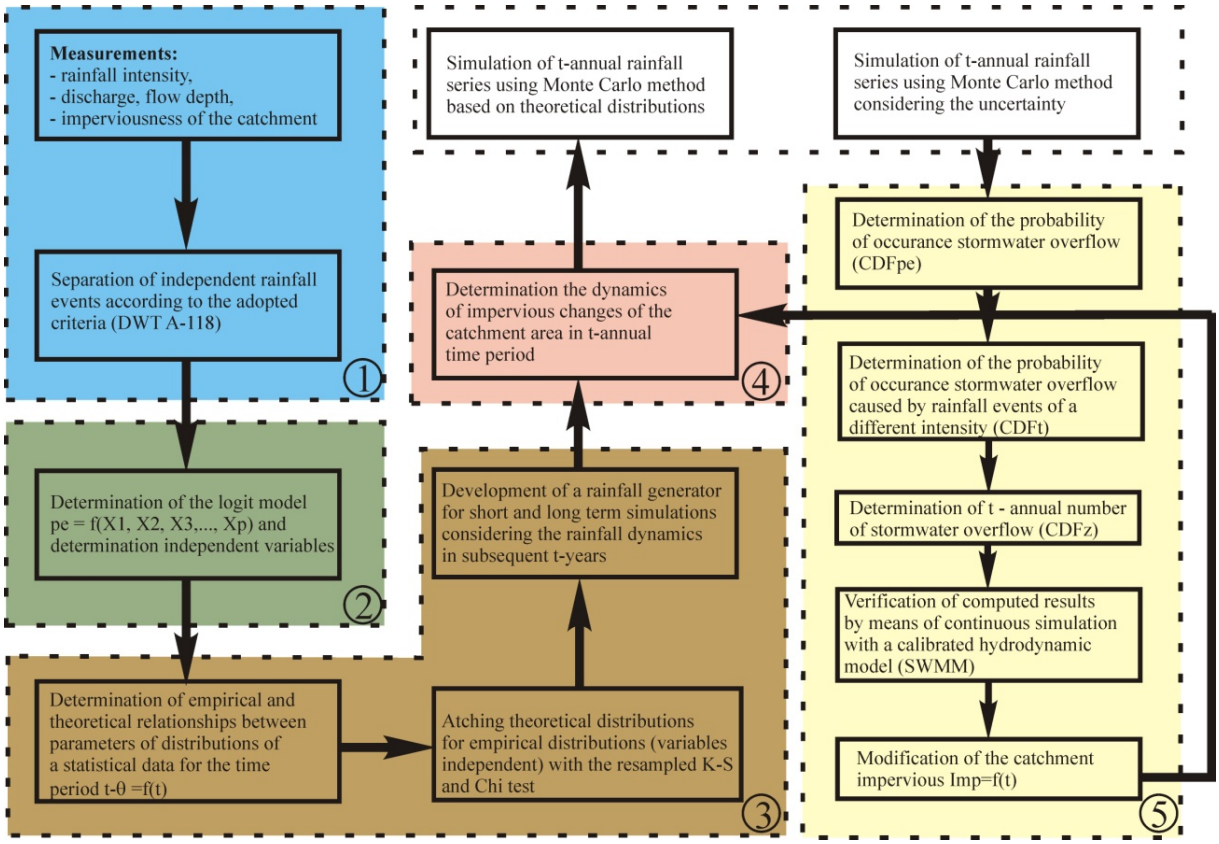

Fig. 2. An algorithm used for the construction of a probabilistic model designed to analyse storm overflow operations: CDF_{pe} – empirical distribution function describing the probability of exceeding the occurrence probability of a storm overflow, CDF_f – empirical distribution function describing the probability of exceeding the occurrence probability of a given number of storm overflow in the designated year, caused by precipitation with a varying average intensity (i), and CDF_Z – a distribution function describing the probability of exceeding the number of storm overflows expected in a period of t years.

The probabilistic model presented in Fig. 2 consists of 5 independent components. Within them, the following modules are determined: prediction of a storm overflow occurring in a single precipitation episode, rainfall depths and changes in their dynamics, urbanisation in a long-term approach and analyses of the produced results. The first component (1) includes the gathering of measured data (intensity of rainfall, flow, filling level, and the impervious

surface of the catchment area). This component serves as a basis for determining a logit model designed to simulate the occurrence of a storm overflow. The second model component model (2) is a synthetic precipitation generator, in which empirical distributions are determined based on the obtained precipitation data and are matched to theoretical distributions. In this component, it is assumed that the values of the parameters in the theoretical distributions exhibit trends that are functions of time; these trends result from changes in precipitation dynamics, which can be caused by climate changes (Bates et al., 2008). This aspect is described in detail in the following part of the paper. The studies included an uncertainty analysis of the identified parameter values of the theoretical rainfall distributions. The third component of the model (3) involves a rainfall simulator based on the Monte Carlo method. The rainfall simulator takes into account the possibility of modelling synthetic precipitation series with changes in precipitation dynamics. The next component (4) includes a module in which rainfall events in consecutive years $[P_1, P_2,\ldots, P_i]_{k=1,2,..,t}$ are assigned impervious area of the catchment. The suggested solution allows the coefficients to have constant values or to be variable as a function of time for the consecutive years covered by the calculations. The final model component (5) constitutes an element in which simulations are performed involving the number of overflows. The impact of the abovementioned factors on the functioning of a storm overflow is analysed based on the produced results. To verify the predictive power of the suggested probabilistic model, continuous simulations are performed based on precipitation data using a calibrated hydrodynamic model.

3.3. Distinguishment of precipitation events and their classification

The precipitation data were acquired from the records of a traditional float pluviograph located in a meteorological station in Kielce city; records from May-October 1961-2005 were

collected. Individual precipitation events were distinguished based on the guidelines of DWA-A 118E (2006). The adopted criteria were 4 h as the minimum dry period length and a minimum precipitation level of 3.0 mm (Fu and Kapelan, 2013; Fu et al., 2014). As a result, 1484 precipitation events were identified in the 1961-2005 period, which means an average of 33 episodes per year. Most of the events involved frontal precipitation (Szeląg et al., 2020). The analysed precipitation events were grouped based on their average intensities. To this end, Sumner's classification (Sumner, 1988) was used as it is the most popular classification method among meteorologists. The precipitation events were grouped into the following categories (WMO, 2012): moderate rain shower (between 2.5 and 10 $mm \cdot h^{-1}$; 416-1667 $L \cdot s^{-1} \cdot ha^{-1}$), heavy shower (between 10 and 50 $mm \cdot h^{-1}$; 1667-8335 $L \cdot s^{-1} \cdot ha^{-1}$) and violent shower (greater than or equal to 50 $mm \cdot h^{-1}$; >8335 $L \cdot s^{-1} \cdot ha^{-1}$). In 1961-2005 in Kielce city, 768, 601, 98 and 17 episodes of light rains, moderate rains, heavy rains and violent rains were identified, respectively.

3.4. Logistic regression

Logistic regression, also called the binomial logit model, constitutes a classification model comprising the methods of supervised learning. This model is used to analyse output and input data of a continuous and binary nature (zero – one). The logit model has been found to be useful in many fields of science, from economy, medicine, microbiology, ecology, and biotechnology to the modelling of objects in drainage networks (Salman and Salem, 2012; Khudhair et al. 2019). The logit model is described by the following equation:

$$p_e = \frac{exp(\alpha_0+\alpha_1 \cdot x_1+\alpha_2 \cdot x_2+\alpha_3 \cdot x_3 \ldots+\alpha_q \cdot x_q)}{1+\exp(\alpha_0+\alpha_1 \cdot x_1+\alpha_2 \cdot x_2+\alpha_3 \cdot x_3 \ldots+\alpha_q \cdot x_q)} \quad (10)$$

where

p_e – the probability of the occurrence of a storm overflow in a precipitation event, α_0 indicates constant term; α_1, α_2, …, α_q – empirical coefficients that are determined using

311 the method of maximum likelihood estimation, and x_q – independent variables including
312 rainfall characteristics and the impervious area of the catchment.
313
314 Equation (10) was used to assess the operation of a storm overflow in a precipitation event.
315 Therefore, a threshold value p_e was established, which, when exceeded, defines the
316 occurrence of an storm overflow. Based on a review of the literature (Szeląg et al., 2020), it
317 was assumed that a storm overflow occurred for values of $p \geq 0.5$, which can be presented as:

318 $$\alpha_0 + \alpha_1 \cdot x_1 + \alpha_2 \cdot x_2 + \alpha_3 \cdot x_3 \ldots + \alpha_q \cdot x_q > 0 \quad (11)$$

319 In an opposite case, i.e., when $p < 0.5$, it was assumed that there was no storm overflow. The
320 assessment of the predictive power of the logistic regression model used the following
321 indicators: sensitivity, denoted by SENS (determines the correctness of the classification of
322 data in a set containing events involving the occurrence of an storm overflow); specificity,
323 denoted by SPEC (determines the correctness of the classification of data in a set constituting
324 cases in which there was no overflow); and calculation error, denoted by R_z^2 (determines the
325 correctness of the identification of event simulations – overflow/no overflow).
326 The logit model was developed based on the results of the rainfall and flow measurements
327 performed in the catchment area in the years 2009-2011 (188 precipitation episodes and 69
328 overflow events were observed) and 2012-2015 (261 and 140 precipitation and overflow
329 events, respectively). Validation of the logit model used 12 independent precipitation events
330 with available measurements of the operation of the storm overflows. To verify the resulting
331 logit model, continuous calculations were performed by means of a calibrated SWMM model
332 based on precipitation in the years 2008-2018. On this basis, the number of storm overflows
333 was determined for consecutive years and compared to the results of the measurements.
334

3.5. Selection of theoretical distributions for the description of precipitation characteristics

Based on the results of the rainfall measurements from 1961-2005, this paper identifies precipitation events in consecutive 30-year periods of the multiannual time interval: 1961-1990, 1962-1991, …, 1976-2005. The following (two-parameter) theoretical distributions were matched with the empirical data (precipitation characteristics determining storm overflow operations): Gumbel, Weibull, Frechet, gamma and log-normal (Adams and Papa, 2000). The assessment of the compliance of the empirical and theoretical distributions were performed using the bootstrap version of Kolmogorov-Smirnov (K-S) test and χ^2 test. The whole procedure of Monte Carlo simulation in goodness of fit testing can be found in the literature (Savapandit and Gogoi, 2015). Proposed number of resampled data is 40 times bigger than number of samples in original data (Wang et al., 2011). There are two types of bootstrap estimation like parametric and nonparametric. The first is more popular in context of goodness of fit testing, in which sample are draw from theoretical distribution with parameters estimated based on original data. In the second one, the samples are draw from original data. The main reason of using resampled version of K-S test was fact that the distribution parameters were estimated form data. The issue with classical Kolmogorov-Smirnov goodness of fit test in such situations widely discussed in the literature (Stephens, 1974; D'Agostino, 2017). 5000 samples were taken for the simulation and a non-parametric approach was used (Savapandit and Gogoi, 2015). The assessment of the compliance of the empirical and theoretical distributions was based on the calculated p-values and critical test values (D) (Fu et al., 2014). In a case in which the calculated values of p were lower than the p-value at the declared significance level (0.05), there was a basis to reject the hypothesis claiming that the analysed theoretical distribution did not comply with the empirical distribution.

3.6. Analysis of changes in precipitation dynamics in a long-term approach

The calculated changes in rainfall dynamics were based on a trend analysis (Ganguli and Coulibaly, 2019) in which a multiannual time interval of 30 years was adopted as a reference unit (DWA-A 118E, 2006). A time series including a period longer than the multiannual time interval, in which the measurements begin in year X_0, can be described by the following relationship:

$$X_0 + k_1, X_0 + k_2, X_0 + k_3, X_0 + k_4, X_0 + k_5, X_0 + k_6, \ldots, X_0 + (t-2), X_0 + (t-1), X_0 + (t = k) \quad (12)$$

where in each subsequent (X_0 + k) year, there was an average of j precipitation events.

The analyses of changes in rainfall dynamics in the multiannual time interval adopted a reference period (time series) including data from within the range of X_0 + (t = k) to X_0 + (t = k) – 30, containing 30·j precipitation events constituting vectors [P_1, P_2,..., P_i]. To analyse the variation in precipitation characteristics in the investigated period, an empirical distribution $f(P_i)_{X0+(t=k)}$ was determined and was paired with the corresponding theoretical distribution $f(P_i)_{X0^{th}(t=k)}$, with the determination of the parameters represented as $\theta_{X0+(t=k),1,2,\ldots,n}$. Subsequently, because the analysed period t was longer than 30 years, another data series was determined for the period between the years X_0 + (t-1) and X_0 + (t-1) – 30. Based on the acquired data, the empirical distribution was determined, followed by the selection of the theoretical distribution $f(P_i)_{X0^{th}+(t-1)}$ and the calculation of the numerical values of the coefficients $\theta_{X0+(t-1),1,2,\ldots,n}$. Subsequently, a time series was determined, including data from the multiannual time interval from X_0 + (t-2) to X_0 + (t-2) – 30, and theoretical distributions $f(P_i)_{X0^{th}+(t-2)}$ were established for the resulting data along with the determination of the values of $\theta_{X0+(t-2),1,2,\ldots,n}$. These models were used to simulate rainfall in the consecutive years covered by the analyses. This is why, to determine the uncertainty of the model predictions, the values

of the standard deviations (σ) of the estimated parameters α_f were determined in the theoretical models $\theta_{X0}{}^{th}{}_{+(t-k),1,2,...,n} = f(\alpha_f, k)$. The adopted approach allows the identification of distribution parameters and therefore an analysis of changes in precipitation dynamics (Kaźmierczak and Kotowski, 2015). By distinguishing 30-year periods within the 50-year precipitation series, these authors suggested the nonlinear variance of the statistical distribution parameters in the analysed timeframe for Wrocław (Poland). Their results were also confirmed by the calculations of Sarhadi and Soulis (2017), who created IDF (intensity-duration-frequency) curves for part of the North American continent, taking into account varying rainfall dynamics. Nonetheless, the relationships identified in this manner were used in a limited capacity to simulate multiannual rainfall series by means of synthetic precipitation generators. Changes in rainfall dynamics in the years 1961-2005 were analysed following the methodology described above.

3.7. Simulator of synthetic rainfall series

The modelling of synthetic rainfall series commonly uses multidimensional probability density distributions generated on the basis of copula functions linking the adopted marginal distributions or modified Monte Carlo generators (e.g., Iman-Conover). If the independent variables (x_p) included in a multidimensional distribution are independent (i.e., their correlations can be omitted), then there is no need to implement linking functions. In this case, each of the variables considered by the model can be modelled independently based on the established theoretical distribution $F(P_i)^{th}$ of the Monte Carlo random number generator. The abovementioned solutions are useful when simulating synthetic rainfall series in a situation in which the dynamics of the changes in the rainfall series over a period covered by the calculations do not change, i.e., when θ_n is constant. Based on the theoretical distribution function $F^{-1}(P_i)$, it is then possible to predict the t–year rainfall series. However, when the

precipitation dynamics change in the period covered by the simulations and the θ_n values in theoretical distributions are different, the need arises to perform analyses on the precipitation dynamics. In this case, the calculations of the *t*-year synthetic rainfall series by means of the Monte Carlo method can be performed for consecutive years based on k combinations of theoretical distributions:

$$G(\mathrm{k}=1,2,3,..,\mathrm{t}) = \begin{cases} \text{when k} = 1 \text{ year}, & [P_i]_j = f(\theta_{X_0+(t-1),1,2,..,n}) \\ \text{when k} = 2 \text{ year}, & [P_i]_j = f(\theta_{X_0+(t-2),1,2,..,n}) \\ \text{when k} = 3 \text{ year}, & [P_i]_j = f(\theta_{X_0+(t-3),1,2,..,n}) \\ & \dots \\ \text{when k} = \text{t years}, & [P_i]_j = f(\theta_{X_0+(t-k),1,2,..,n}) \end{cases} \quad (13)$$

assuming that

$$j(\mathrm{k}=1,2,3,\dots,\mathrm{t}) = \text{const and } \theta^{th}_{X_0+(t-k),1,2,..,n} = f(a_{f,}\ \mathrm{k}) \quad (14)$$

where

j, k, P_i, X_0, n, and α_f are denoted according to the symbols in formulas (1-12).

Based on the results of Suligowski (2004), who showed for selected Polish cities that the variability of the average rainfall intensity in a rainfall event (*i*) over a multi-year period can be described by a log-normal (two-parameter) distribution and assuming that its parameters (μ, σ) can be expressed as a polynomial function depending on time (t), the following system of equations for modeling rainfall series was obtained:

$$\begin{cases} F(x) = \frac{1}{2} + \frac{1}{2} \cdot erf\left(\frac{\ln(x-\mu)}{\sigma \cdot \sqrt{2}}\right) \\ x \in \langle 0; 1 \rangle \\ \mu = a_1 \cdot t^2 + a_2 \cdot t + a_0 \\ \sigma = b_1 \cdot t^2 + b_2 \cdot t + b_0 \\ \text{for: } t = 0, 1, 2, 3, \dots, k \end{cases} \quad (15)$$

where

F(x) – cumulative log-normal distribution, x – values of pseudo-random numbers modeled from theoretical distributions, μ i σ – parameters of the theoretical distribution, a_1, a_2, a_0, b_1, b_2, b_0 – coefficients of the selected models for modelling μ, σ. Assuming

the values of t, the parameters of the distribution F(x) for the following years are calculated and precipitation simulations are performed.

The values of the parameters a_1, a_2, a_0, b_1, b_2, b_0 in Eq.15 were estimated using the least squares method, while the Akaike Information Criterion (AIC) was applied for the assessment of the models $\mu = f(t)$ and $\sigma = f(t)$. The results of calculations of μ and σ polynomial parameters are given in Appendix B.

The computational algorithm for simulating the t-year rainfall series as described above was used in the paper to model the number of storm overflows. The simulation of synthetic rainfall series for consecutive years involved the N-sampling of M precipitation events in a year, resulting from the established theoretical distributions. Due to the strong correlation between the precipitation intensity (i) values in consecutive periods t (as indicated in the paper of Kupczyk and Suligowski, 1997 – Appendix C), the Iman-Conover (I-C) method was used in the simulations of multiannual synthetic rainfall series. In this method, the assessment of the correlations among z variables is based on the value of Spearman's correlation. The results of the application of the I-C method are discussed in detail in the paper by Iman and Conover (1982), and these results are also cited in the Appendix D. This method is useful when simulating numerous independent variables (even exceeding 10) that are correlated with each other in a model. A good example of this includes complex technical facilities such as wastewater treatment plants, power plants, industrial plants, elements of machines such as gas turbines, and processes (Bixio et al., 2002; Talebizadeh et al., 2014; Forrester and Keane, 2017; Maronati and Petrovic, 2019). To limit the number of samples, the Monte Carlo simulations used the Latin Hypercube method (LH).

To take into account the uncertainty of the identified parameters of the theoretical distributions, it was initially necessary to perform P simulations (500 samples were used in the paper) of theoretical distribution parameters $N(\mu_s, \sigma_s)$. On their basis, calculations of N

457 samples for M precipitation events were performed from distributions describing the
458 precipitation characteristics of a given event. The obtainted results were entered into equation
459 (10), and the probability of storm overflow with the annual number of storm overflow was
460 calculated by establishing the empirical distribution functions (CDF_{pe}, CDF_Z). Moreover, a
461 95% confidence interval was determined for the established empirical percentiles. A detailed
462 description of the method used to analyse uncertainty is presented in the paper by Grum and
463 Aalderink (1999).
464
465 **3.8. A catchment area urbanisation process within a time horizon**
466 The description of long-term changes in the land development of a catchment area, which are
467 a direct cause of increases in land imperviousness, used an original model in the following
468 form:

469
$$\mathrm{Imp}(t) = \begin{cases} \mathrm{Imp}_0 + (\mathrm{Imp}_m - \mathrm{Imp}_0) \cdot \left(\frac{t}{t_{cr}}\right)^a & \text{for} \quad t_{cr} \geq t \geq 0 \\ \mathrm{Imp}_e + (\mathrm{Imp}_m - \mathrm{Imp}_e) \cdot \left(\frac{t_{sust} - (t - t_{cr})}{t_{sust}}\right)^b & \text{for } t_{cr} + t_{sust} \geq t \geq t_{cr} \end{cases} \quad (16)$$

470 where
471 t_{cr} – the period of an increase in the impervious area of the catchment; t_{sust} – the period of
472 optimal shaping of the impervious area of the catchment; Imp_0 – the initial impervious
473 area of the catchment; Imp_m – the maximum impervious area of the catchment; Imp_e –
474 the impervious area of the catchment after a period of t_{cr} + t_{sust}, and a, b – empirical
475 coefficients describing the dynamics of urbanisation in the catchment area.
476
477 The developed model provides high flexibility when studying the relationships among the
478 phase of an increase in the impervious area of the catchment (this is allowed by the
479 coefficients a and b) and actions aimed at compensating for the insufficient retention volume
480 of the catchment area within a specified timeframe. This allows the deliberate and rational

management of the catchment area in compliance with the principles of sustainable development and a bio-circular economy.

The performed analyses of the functioning of a storm overflow took into account the impact of the dynamics of changes in the impervious area of the catchment within the given period ($t_{cr} + t_{sust}$) on the number of storm overflows. In the performed calculations, the values of t_{cr} and t_{sust} changed over a period of 1-5 years, and the timeframe of the simulations ($t_{cr} + t_{sust}$) did not exceed 10 years.

3.9. Verification of the probabilistic model – continuous simulations using a hydrodynamic model

A hydrodynamic model of an urban catchment area developed in SWMM 5.1 software was used to verify the probabilistic model of storm overflow operations. To this end, continuous simulations were performed based on 30-year rainfall series for consecutive computational scenarios.

The hydrodynamic model studied in the paper consists of 92 partial catchment areas, 200 manholes and 72 sewers. The sizes of the partial catchment areas vary from 0.12 ha to 2.10 ha. As result of the calibration procedure, it was determined that the value of Manning's roughness coefficient of the sewer was $n_{sew} = 0.018$ $m^{-1/3} \cdot s$, the Manning roughness coefficient and retention of impervious areas were $n_{imp} = 0.025$ $m^{-1/3} \cdot s$ and $d_{imp} = 2.50$ mm, and the runoff path width was calculated as $W = \alpha \cdot A^{0.50}$ where $\alpha = 1.35$. The results of the simulation (Szeląg et al., 2016) demonstrated that, for the abovementioned combinations of coefficients, the developed model is characterised by satisfactory predictability.

Two independent computational approaches were used during the verification of the probabilistic model. The first approach included a multiannual time interval (30 years) established based on equation (12), and the model performed continuous simulations of the

number of storm overflows for various impervious area of the catchment (Imp = 0.3-0.5). In the abovementioned solution, 30-year precipitation series were identified within the time series, i.e., 1961-1990, 1962-1991, 1963-1992, etc., which, in the following step, were entered into the SWMM model to simulate the annual number of storm overflows.

In the second approach, calculations of the multiannual number of storm overflows were performed while taking into account the changes in imperviousness over the consecutive years. In this case, it was necessary to simultaneously prepare numerous models of the catchment area, in which different values of the impervious area of the catchment, assigned to the consecutive years covered by the calculations, were defined based on equation (12). A layout of the construction of a model for continuous simulations in which the characteristics of the catchment area change in a dynamic system over consecutive years is presented in Fig. 3.

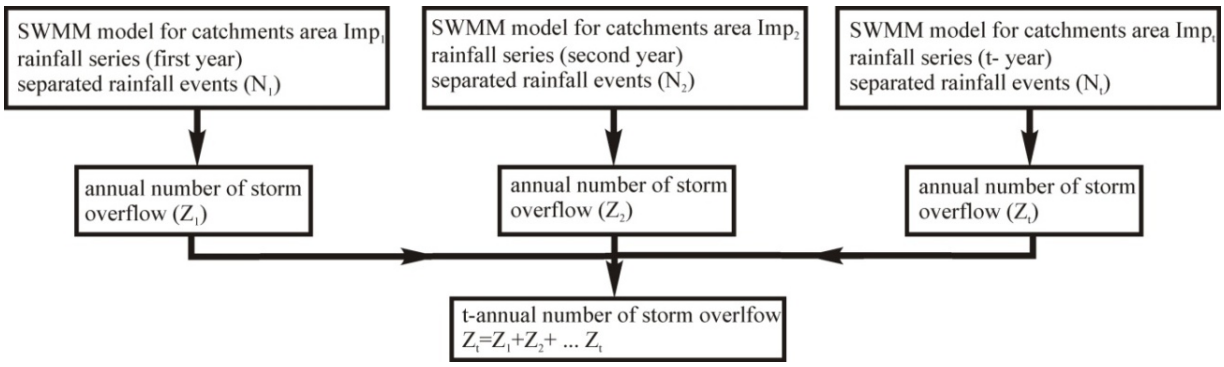

Fig. 3. Scheme of the construction of a hydrodynamic model used to simulate the number of storm overflows in a period of t years.

Based on the suggested computational algorithm (Fig. 3), calculations of the number of storm overflows were performed for a period of t = 10 years.

4. Results and discussion

4.1. The logistic regression model

Based on precipitation data and changes in the impervious area of the catchment, the following logit model was developed:

$$p_e = \frac{\exp(0.352\, i + 3.928\, \mathrm{Imp} - 5.298)}{1+\exp(0.352\, i + 3.928\, \mathrm{Imp} - 5.298)} \quad (17)$$

where

p_e – the probability of the occurrence of a storm overflow, Imp – the impervious area of the catchment, and i – the average rainfall intensity ($L \cdot s^{-1} \cdot ha^{-1}$).

The established logit model is characterised by high accuracy of measurement data. This is indicated by the following values: SPEC = 87.22% (out of 209 storm overflows, 182 precipitation episodes were identified properly), SENS = 87.87% (out of 240 precipitation episodes, 211 events were classified properly), and R_z^2 = 87.55% (out of 449 events, the operation of the storm overflow was identified properly in 393). Validation of the resulting logit model was also performed. This was done using 12 independent precipitation events. The completed calculations indicate that out of 7 storm overflows, the logit model properly predicted 6 events; for 5 measured precipitation events, in the absence of an overflow event, the results of the calculations using the logit model were similar for all episodes. To verify the logit model, continuous simulations of the annual number of storm overflows (Z_{SWMM}) were performed by means of a calibrated hydrodynamic model of the catchment area. The results of calculations are presented in tab. 1.

Tab. 1. Results of the verification of the logit model

Year	Imp	N	Z_{mes}	Z_{logit}	Z_{SWMM}
2008	33	43	15	12	16
2009	33	47	16	17	16

2010	35	47	18	15	19
2011	38	51	20	21	20
2012	38.3	36	-	16	15
2013	38.6	41	-	17	15
2014	39	44	-	22	23
2015	40	58	24	21	24
2016	41.3	44	20	22	20
2017	45	38	20	18	20
2018	50	42	20	22	20

548 Z_{mes} – actual number of storm overflows, Z_{logit} – number of overflows determined by the logit model, Z_{SWMM} –
549 number of storm overflows resulting from continuous simulations.

550

551 Based on the data included in the table, it can be concluded that the annual numbers of storm
552 overflows determined by means of the logit model and those based on the continuous
553 simulations are highly compliant. The maximum difference in the annual number of storm
554 overflows between the results from the SWMM model and those from the logit model equals
555 3. An identical maximum difference was achieved between the measurements and the results
556 of the logit model. As indicated above, the established logistic regression model can be
557 applied to further analyses.
558 To allow the interpretation of the individual terms in equation (17), they were written in a
559 simplified form:

560 $$0.395\, i + 3.928\, \mathrm{Imp} - 5.498 \geq 0 \qquad (18)$$

561 By normalising equation (18) (Thorndahl and Willems, 2008, Szeląg et al., 2020), assuming
562 that, in the analysed period, Imp ≈ 0.40, the following relationship was produced:

563 $$i + \frac{3.928}{0.395} \cdot 0.40 - \frac{5.498}{0.395} = i + 3.98 - 13.92 \geq 0 \qquad (19)$$

564 which finally resulted in:

565 $$i - 9.94 \geq 0 \qquad (20)$$

566 In equation (20), the value of the constant term (i.e., 9.94) is similar to the value of the
567 average rainfall intensity (i_0 = 10.82 $L \cdot s^{-1} \cdot ha^{-1}$) that determines the occurrence of a storm
568 overflow event in the analysed catchment area (Szeląg et al., 2019). According to the

literature (Thorndahl and Willems, 2008), it can be assumed that the value i_0 is a function of the physical-geographical characteristics of the catchment area; however, this aspect has not yet been studied in catchment areas with various characteristics, and it thus requires further detailed analyses. This is important from the point of view of the construction of a universal model for predicting the occurrence of a storm overflow event. Attention should also be paid to the fact that the suggested approach, when compared to the traditional approach (P_t, t_r) discussed in numerous papers (Grum and Aalderink, 1999; Thorndahl and Willems, 2008; Szeląg et al., 2019), constitutes a significant simplification at the construction stage of the model and simulations, which constitutes its major advantage.

4.2. Establishing the theoretical distributions of independent variables

Based on the distinguished precipitation events, empirical distributions of the rainfall intensity values were determined for the consecutive periods of the multiannual time interval (30 years) in the resulting time series. Subsequently, theoretical distributions were matched with the resulting empirical distributions. Tab. 2 presents the critical test probability values of the resampled Kolmogorov–Smirnov (K-S) and χ^2 tests, which resulted in the best match with the empirical data. The results of the K-S and χ^2 test calculations for the remaining statistical distributions are presented in the Appendix E.

Tab. 2. Results of K-S* and χ^2 test calculations and the values of the matching parameters (μ, σ) in the theoretical distributions

Multiannual time interval	Distribution	p(K-S)	p(χ^2)	Parameter (average value)		Standard deviation	
		p-value	p-value	μ_s	σ_s	$\sigma_{\mu s}$	$\sigma_{\sigma s}$
1961-2005	lognorm	0.310	0.251	1.966	0.856	0.009	0.017
1961-1990	lognorm	0.210	0.187	1.883	0.837	0.034	0.010
1962-1991	lognorm	0.203	0.195	1.884	0.829	0.017	0.012
1963-1992	lognorm	0.105	0.092	1.881	0.842	0.020	0.017
1964-1993	lognorm	0.119	0.121	1.892	0.841	0.039	0.009
1965-1994	lognorm	0.237	0.221	1.881	0.845	0.023	0.008

1966-1995	lognorm	0.275	0.224	1.905	0.851	0.029	0.018
1967-1996	lognorm	0.303	0.258	1.915	0.860	0.027	0.005
1968-1997	lognorm	0.208	0.210	1.928	0.862	0.028	0.014
1969-1998	lognorm	0.141	0.121	1.922	0.863	0.027	0.016
1970-1999	lognorm	0.247	0.214	1.916	0.861	0.023	0.010
1971-2000	lognorm	0.142	0.123	1.918	0.865	0.019	0.012
1972-2001	lognorm	0.331	0.257	1.933	0.866	0.023	0.018
1973-2002	lognorm	0.311	0.287	1.948	0.859	0.025	0.012
1974-2003	lognorm	0.132	0.116	1.963	0.853	0.020	0.009
1975-2004	lognorm	0.398	0.321	1.989	0.856	0.029	0.018
1976-2005	lognorm	0.100	0.109	1.991	0.857	0.020	0.015

590 μ_s, $\sigma_{\mu s}$ – average value and standard deviation of the μ values, resulting in a normal distribution in the form of
591 N(μ_s, $\sigma_{\mu s}$) for simulating the uncertainty of parameter μ_s of the theoretical distribution; and
592 σ_s, $\sigma_{\sigma s}$ – average value and standard deviation of the σ values, resulting in a normal distribution in the form of
593 N(σ_s, $\sigma_{\sigma s}$) for simulating the uncertainty of parameter σ_s of the theoretical distribution.
594

595 An analysis of the data in Tab. 2 indicates that the empirical data are best matched by the log-
596 normal distribution, and the standard deviation values in relation to the established values of
597 parameters μ_s and σ_s do not exceed 2.2% (the maximum error in the data from 1964-1993). In
598 the case of parameter σ, it was concluded that the parameter reaches its maximum value in the
599 period from 1969 to 1998 and then falls. The resulting relationships are presented in Figs. 4a
600 and 4b.

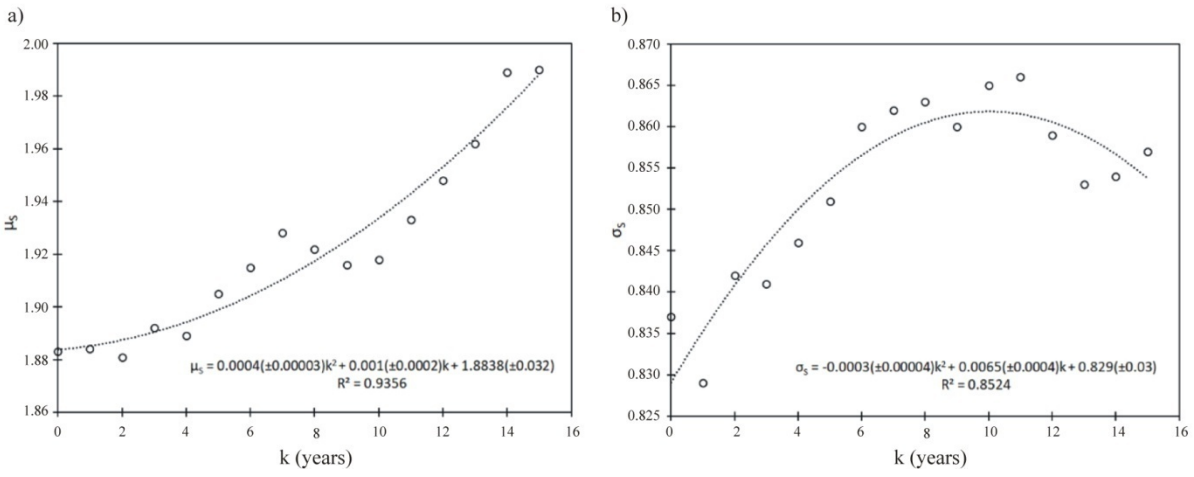

601

602 **Fig. 4.** Variability of the values of parameter μ **(a)** and parameter σ **(b)**, measured and interpolated for
603 the consecutive periods of the multiannual time interval.

604

When analysing the shape of the curves (measurements and interpolation), it can be concluded that the adopted second-degree polynomials reflect the changes in the μ_s and σ_s coefficients in the log-normal distributions with a satisfying accuracy. The resulting relationships can constitute a basis for determining the values of μ_s and σ_s in consecutive years. The presented approach is confirmed by the literature (Kaźmierczak and Kotowski, 2015), and it is used in computational experiments involving changes in precipitation dynamics in a multiannual approach. In the following sections, calculations of the probability of a storm overflow in a given year (including multiannual calculations) and the number of storm overflows were conducted using the empirical values of μ and σ derived from the theoretical distributions (tab. 2).

4.3. Impact of the uncertainty of the parameters of the statistical distributions of precipitation on calculation results involving the operations of storm overflows

The performed calculations included an analysis of the impact of the uncertainty of the identification of the parameters of statistical distributions (tab. 2) on the probability of the occurrence of an overflow event and on the simulated annual number of overflows. The first scenario involved modelling the impact of the uncertainty of the estimation of the parameters in distributions describing the average intensity of rainfall (tab. 2). In the second scenario, the values of the parameters in the theoretical distributions were calculated using regression models. The uncertainty of the parameters identified in the statistical distributions was modelled based on the calculated average values of the parameters and the calculated standard deviations. The results of the calculations of the empirical distribution functions (CDF_{pe}, CDF_{Zt}) based on the theoretical distribution (1975-1994) and Imp = 0.50, taking into account the uncertainty (average value), with indicated 95% intervals, are presented in Fig. 5.

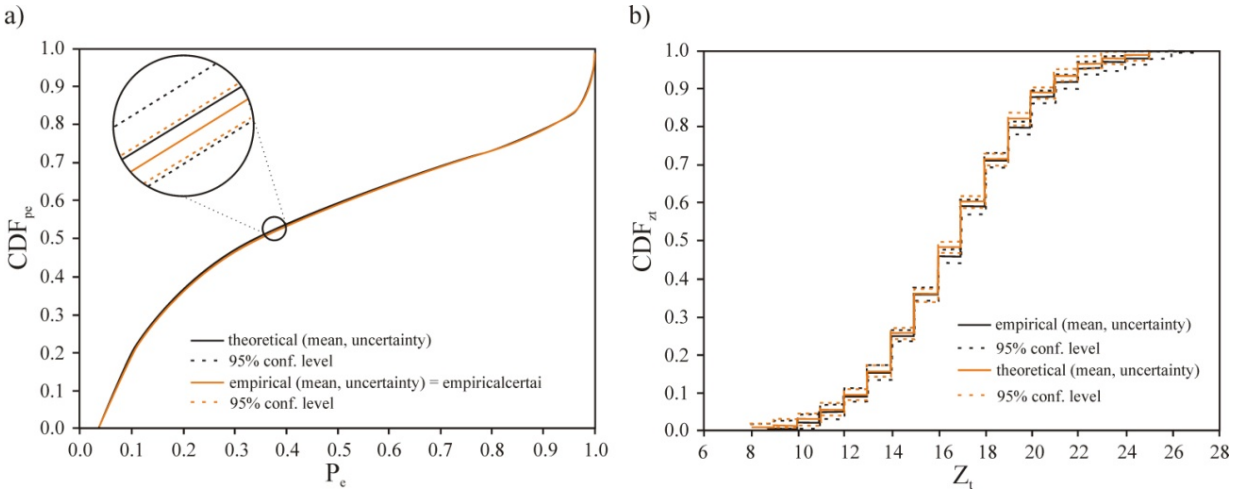

629

630 **Fig. 5.** Empirical distribution functions calculated while taking into account the uncertainty of the
631 estimation of the theoretical distribution parameters, describing the probability of exceeding: a) the
632 probability of the occurrence of an storm overflows (p_e); b) the annual number of storm overflows (Z_t).

633

634 The resulting distribution functions were compared to the simulation results for the case that
635 omitted the uncertainty of estimated parameters in the statistical distributions of rainfall
636 characteristics.

637 Based on the resulting curves (Figs. 5a and 5b), it was concluded that the uncertainty of the
638 estimation of the parameters in the statistical distributions of rainfall had a minor impact on
639 the results when calculating the probability of the occurrence of a storm overflows-event and
640 the annual number of storm overflows. This was confirmed by the established ranges of 95%
641 confidence intervals in relation to the modelled variables, i.e., p_e and Z_t. Based on the
642 resulting curves (Fig. 5a) for the period of 1961-1990, it was concluded that the values of p_e
643 that were determined based on the parameters of the theoretical distributions of precipitation
644 by means of the relationships $\mu_s = f(t)$ and $\sigma_s = f(t)$ are higher than those obtained in the results
645 of the calculations that were based on the empirical parameters (tab. 2, columns 7 and 8). This
646 is reflected by the calculated distribution functions representing the yearly number of storm
647 overflows (Fig. 5b). For the assumed number of storm overflows n each year (Z_t), the

resulting percentile values were higher for the case in which the distribution parameter values were estimated based on the relationships $\mu_s = f(t)$ and $\sigma_s = f(t)$. An analysis of the established 95% confidence intervals demonstrated that, in the scenario in which the parameters of the statistical distributions of rainfall were estimated based on the relationships $\mu_s = f(t)$ and $\sigma_s = f(t)$, the resulting parameters were lower than the values of the empirical parameters (tab. 2). Referring to the remaining rainfall distributions (periods: 1962-1991 to 1976-2005), it was proven that the values of p_e (percentile 0.50) calculated based on the empirical data and based on the relationships $\mu_s = f(t)$ and $\sigma_s = f(t)$ differed by a maximum of 3%. Therefore, it can be concluded that the uncertainty of parameter estimations in the statistical distributions had little impact on the values of p_e and Z_t. At the same time, this confirms the credibility of the produced results of the calculations of variables covered by the simulations.

4.4. The impact of changes in precipitation dynamics and urbanisation on the operation of a storm overflow

The impacts of the imperviousness of the catchment area and rainfall dynamics were analysed based on the established logit model and the theoretical distributions (a simulation of a single value of rainfall intensity was performed 2500 times using the LH method) of average rainfall intensity in the consecutive periods of the multiannual time interval (tab. 3). For example, the theoretical distributions of rainfall selected for the analyses originated from the periods from 1961 to 1990 and from 1975 to 2004 (parameters were calculated from the statistical distributions based on the data from tab. 2). By means fitting the theoretical distributions of rainfall intensity, a simulation was performed using the LH method, and the probability of the occurrence of storm overflow was determined for the adopted impervious area of the catchment Imp = 0.3-0.5. The resulting CDF_{pe} curves are presented in Fig. 6.

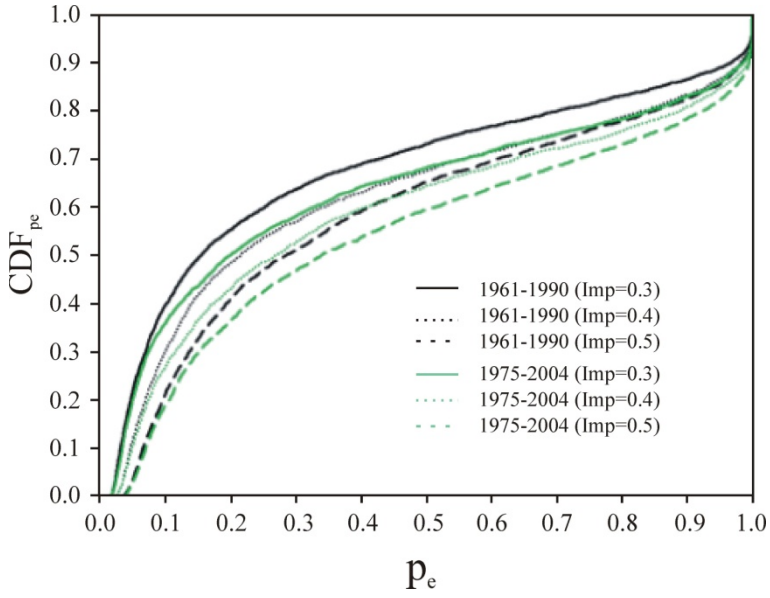

672

673 **Fig. 6.** The impacts of changes in precipitation dynamics in the consecutive periods of the multiannual
674 time interval and of the impervious area of the catchment on the probability of the occurrence of a
675 storm overflow event (p_e).

676

677 Based on an analysis of the shape of the curves (Fig. 6), it was concluded that both the
678 urbanisation of the catchment area and the dynamics of rainfall had significant impacts on the
679 probability of the occurrence of a storm overflow event (p_e). For example, the values of the
680 0.5 percentile, determined based on the theoretical distribution, for the periods from 1961 to
681 1990 and from 1975 to 2004 at Imp = 0.30 are 0.150 and 0.194, respectively. The results
682 yielded in this manner confirm the impact of changes in rainfall dynamics in a multiannual
683 approach on p_e, and these results are confirmed by the analyses of Bendel et al. (2013). By
684 applying the results of the precipitation forecasts of a 30-year period, the researchers indicated
685 an increase in the occurrence frequency of storm overflows based on calculations using a
686 hydrodynamic model of the studied catchment area. Moreover, an analysis of the
687 abovementioned curves indicates that, for theoretical distributions determined based on
688 precipitation data from the period from 1961 to 1990, an increase in the imperviousness of the
689 catchment area from Imp = 0.30 to Imp = 0.50 leads to an increase in the probability

(Arnbjerg-Nielsen et al., 2013) of an storm overflow event from $p_e = 0.150$ to $p_e = 0.271$. The results of calculations demonstrate that both the urbanisation of the catchment area and the dynamics of changes in rainfall in a multiannual approach have a considerable impact on the operation of a storm overflow, with a strong interaction occurring between them (Wu et al., 2013). This is reflected by the value of the 0.5 percentile derived from the theoretical distributions for the period from 1961 to 1990 and Imp = 0.50, as well as the value derived from the theoretical distributions for the period from 1975 to 2004 and Imp = 0.40; these values are almost identical and are equal to 0.268 and 0.265, respectively.

4.5. The impact of the dynamics of changes in precipitation on the annual number of storm overflows with respect to the classification of precipitation

Calculations of the annual number of storm overflows were performed based on the established theoretical distributions (a simulation of 33 precipitation events in a given year was performed 2500 times by means of the LH method) for the consecutive periods of the multiannual time interval (tab. 2) and by the developed logit model for the value Imp = 0.45. At the same time, continuous simulations were performed by means of a calibrated hydrodynamic model of the catchment area for the respective 30-year rainfall periods. The results of the performed analyses are presented in Fig. 7.

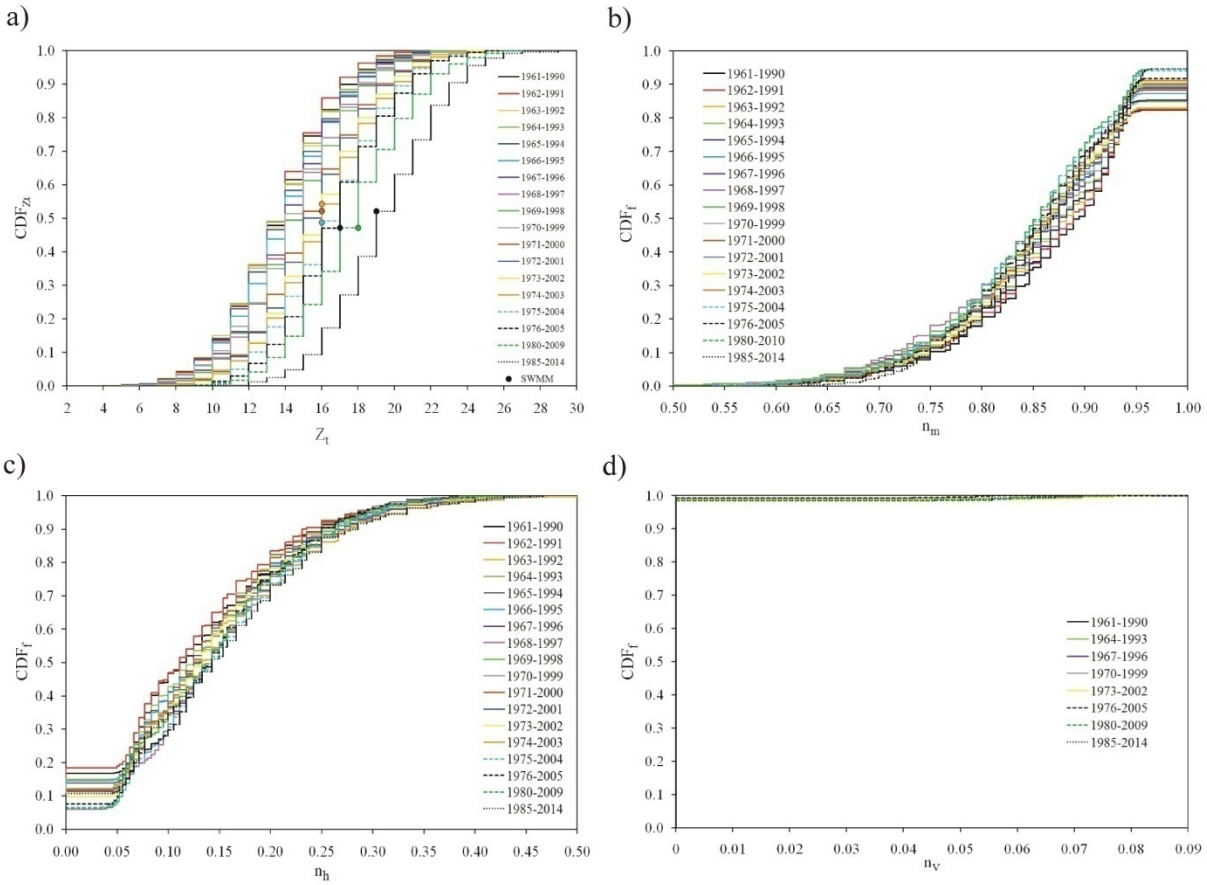

708

709 **Fig. 7.** The impact of the dynamics of changes in precipitation in the consecutive periods of
710 a multiannual time interval on **a)** the annual number of storm overflows; **b-d**) the probability of the
711 occurrence of a storm overflow in a given year caused by a moderate (b), heavy (c) or violent
712 downpour (d).

713

714 Based on the resulting curves, it can be concluded that changes in precipitation dynamics in
715 the consecutive periods of the multiannual time interval from 1961 to 1975 had significant
716 impacts on the annual number of storm overflows. The shape of the resulting curves indicates
717 an increase in the calculated number of storm overflows based on the theoretical distributions
718 derived from the precipitation data from the consecutive periods of the multiannual time
719 interval (starting from 1961). This is confirmed by the values of the resulting 0.5 percentiles.
720 For example, the annual number of storm overflows for the data from the period from 1961 to
721 1990 was 13, while the value determined for the period from 1976 to 2005 equalled 16. The

722 resulting pattern can also be observed in the values of the remaining percentiles. For example,
723 for the 0.05 and 0.95 percentiles, the annual numbers of storm overflows determined for the
724 period from 1961 to 1990 amounted to 9 and 18, and those for the period from 1976 to 2005
725 amounted to 12 and 22, respectively. The results of the simulations indicate the impacts of
726 climate change on the operation of sewage networks, including on the objects existing within
727 the sewage networks, such as storm overflows. These results are confirmed by the analyses
728 performed by Bendel et al. (2013), who, by using a calibrated model of the studied catchment
729 area and predicting rainfalls by means of the NiedSim-Klima model, demonstrated an
730 increase in the number of storm overflows in an urbanised catchment area in Baden-
731 Württemberg. These results are also confirmed by the analyses performed by Tavakol-Davani
732 et al. (2016), who, by performing simulations using a calibrated model for the catchment area
733 of Toledo (Canada) based on multiannual precipitation forecasts, demonstrated a 15% impact
734 of the annual number of overflows over a 30-year period. A similar increase in the number of
735 storm overflows for a 30-year period was also confirmed by Abdellatif et al. (2015), who
736 performed similar simulations for the catchment area of Crewe in northern England. It should
737 be noted that the results of continuous simulations using a calibrated model of the studied
738 catchment area fall within the range of probabilistic solutions, which indicates the
739 applicability of the model to predicting the annual number of storm overflows.
740 The probability of the occurrence of an storm overflow in a given year caused by rainfall with
741 a varying intensity was analysed to supplement the abovementioned results and investigate
742 the impact of the dynamic process of rainfall changes on the operation of a storm overflow.
743 The results of the calculations are presented in Figs. 7b-d. On the basis of these results, it was
744 concluded that storm overflows in consecutive years occurred as a result of various types of
745 precipitation: moderate, heavy and violent. Moreover, the resulting curves indicate that a
746 change in rainfall dynamics in the consecutive years of the 1961-1975 period led to a decrease

747 in the probability of the occurrence of an storm overflow caused by a moderate downpour
748 (Fig. 7b), as confirmed by the values of the calculated percentiles. In contrast, the probability
749 of the occurrence of a storm overflow caused by a violent or heavy downpour increased
750 correspondingly. To date, this aspect has not been addressed by researchers involved in the
751 modelling of storm overflows. Based on the results of continuous measurements of
752 precipitation and a calibrated hydrodynamic model for Innsbruck city, Jean et al. (2019)
753 analysed the possibility of determining precipitation characteristics for the design of an
754 overflow. However, to a limited extent, these authors took into consideration aspects related
755 to the identification of rainfall, which could have affected the final results of the calculations
756 and problems with the interpretation of the resulting relationships.
757 The results yielded in this paper can be used to identify the occurrence of a storm overflow
758 based solely on precipitation intensity, depending on changes in rainfall dynamics during the
759 multiannual time interval. However, one should aim to generalise the produced results;
760 therefore, these analyses should cover broader areas (Guo and Urbonas, 2002; De Paola and
761 Ranucci, 2012).
762

763 **4.6. The impact of urbanisation and changes in precipitation dynamics on the annual**
764 **number of storm overflows**

765 By proceeding in accordance with the developed computational algorithm, based on the logit
766 model (equation 17) and the established parameters of the theoretical distributions for the
767 years 1961-1990 and 1975-2004, the annual numbers of storm overflows (Z_t) were
768 determined for the adopted values of Imp = 0.3-0.5 (Fig. 8). The calculations used synthetic
769 precipitation series (2500 samples), assuming 33 episodes per year. To assess the
770 predictability of the model, continuous simulations were performed on the basis of the
771 adopted time series.

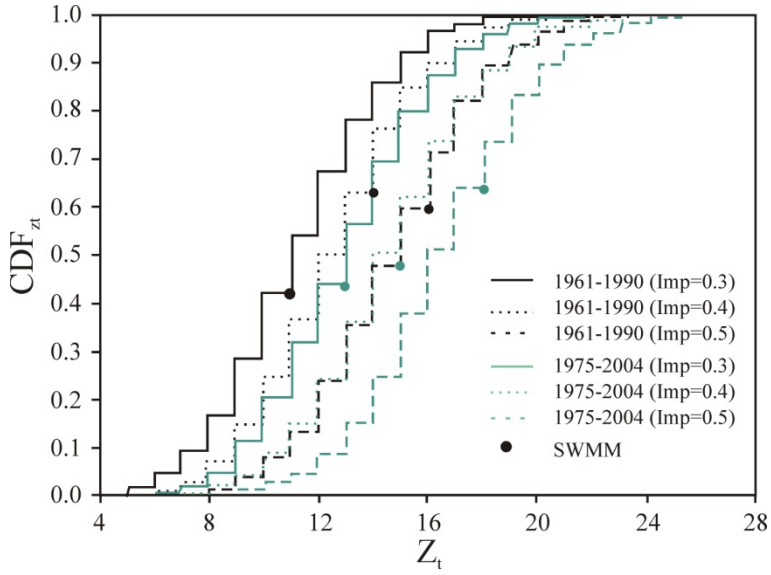

772

773 **Fig. 8.** The impacts of changes in precipitation dynamics in the periods from 1961 to 1990 and 1975 to
774 2004 and of the impervious area of the catchment (Imp) on the annual number of storm overflows (Z_t).

775

776 The resulting curves (Fig. 8) confirm the relationship shown in Fig. 6 and present the impact
777 of changes in rainfall dynamics in the analysed periods of the multiannual time interval. An
778 analysis of the shape of the curves of Fig. 8 indicates the significant impact of the
779 imperviousness of the catchment area on the annual number of storm overflows. For both the
780 CDF_{Zt} curve derived from precipitation data from the period from 1961 to 1990 and that from
781 1975 to 2004, an increase in the imperviousness of the catchment area of $\Delta Imp = 0.1$ (from
782 Imp = 0.3 to Imp = 0.4) led to an increase in the annual number of storm overflows by 1 for
783 the 0.5 percentile (from 11 to 12 in the period from 1961 to 1991 and from 13 to 14 in the
784 years 1975-2004). Similar relationships were also derived for the 0.95 percentile. These
785 results are confirmed by the calculations performed by other authors (Kirshen et al., 2014;
786 Fortier and Maihlot, 2015; Tavakol-Davani et al., 2016) by means of calibrated hydrodynamic
787 models of urban catchment areas. These authors observed that the impacts of changes in
788 precipitation dynamics relative to the multiannual time interval led to an increase in the
789 number of storm overflows of no less than 10%. Analogical conclusions were drawn by

Szeląg et al. (2019), who, like the abovementioned researchers, focused solely on the impact of changes in the impervious area of a catchment on the number of storm overflows; the aspect related to rainfall dynamics over time was neglected.

From a practical point of view and regarding the usefulness of the proposed model, it is important that the results of continuous simulations using the hydrodynamic model for the period from 1962 to 1991 and the period from 1975 to 2004 fall within the scope of the probabilistic solution, which confirms the correctness of the approach proposed in the paper. Moreover, the values of the 0.5 percentiles derived from the SWMM model and the proposed probabilistic model are highly compliant, which confirms the credibility of the produced calculation results.

4.7. The impact of urbanisation dynamics on the multiannual number of storm overflows

The performed analyses included consideration of the impact of urbanisation dynamics in the studied urban catchment area in the period covered by the studies, which corresponded to t_{cr} = 10 years. Using the developed logit model, the theoretical distribution of precipitation intensity values (1961-2004), and the model for predicting the imperviousness of the catchment area (equation 17), while assuming that $Imp_0 = 0.33$ and $Imp_m = 0.55$, simulations of the precipitation characteristics (i) of the events were performed by means of the LH method (2500 samples). The following computational scenarios were analysed to assess the impacts of urbanisation dynamics on the number of storm overflows: I (a = 1.00), II (a = 0.40), III (a = 2.40), IV (a = 0.25) and V (a = 2.80). The calculations served as a basis for determining the multiannual number of storm overflows (Z_t) and the probability of an storm overflows caused by downpours of the following intensities: moderate (n_m), heavy (n_h) and

violent (n_v). The simulation results yielded for the abovementioned assumptions are presented in Fig. 9a-c.

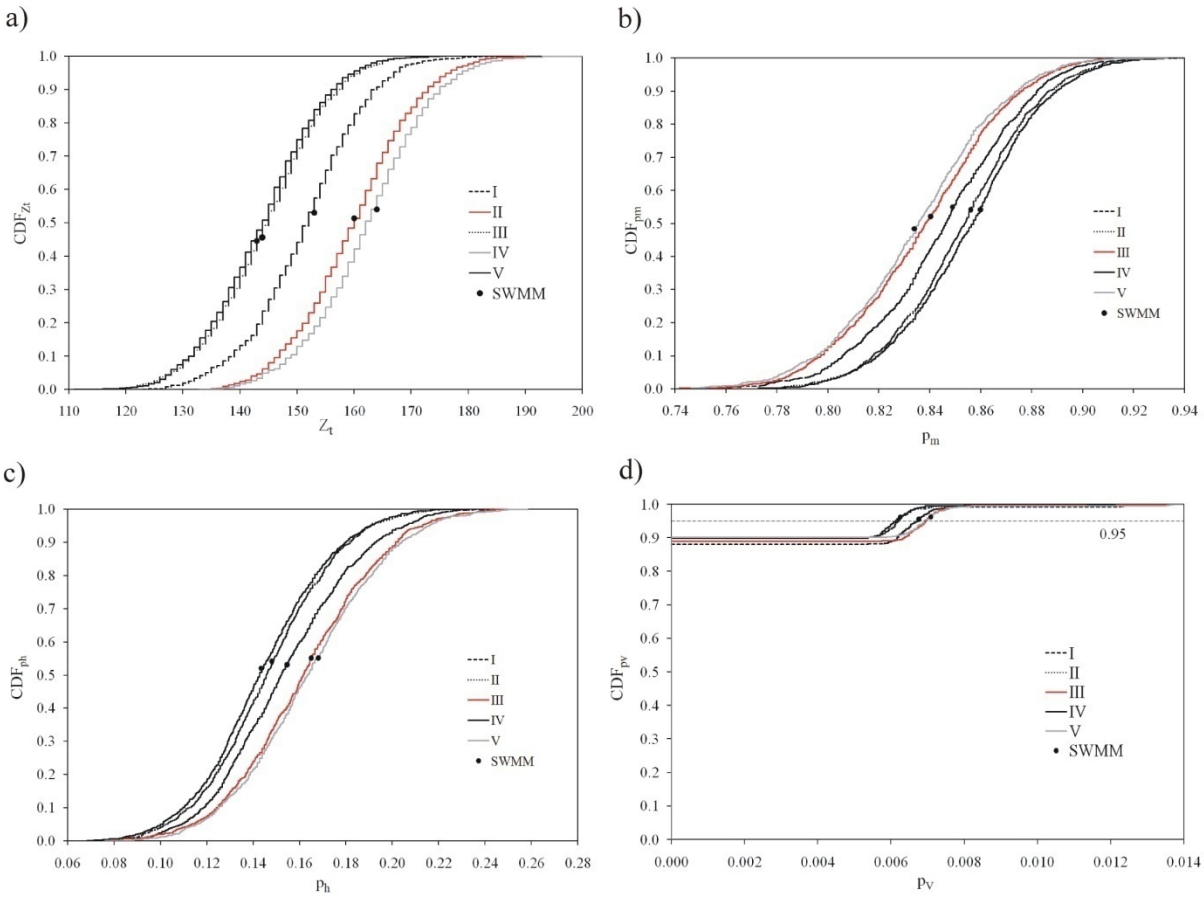

Fig. 9. Selected characteristics of storm overflows for scenarios I, II, III and IV of the dynamics of changes in the impervious area: **(a)** the probability of exceeding a 10-year number of storm overflows (Z_t); **(b-d)** the probability of the occurrence of a storm overflow (t = 10 years) caused by a moderate (b), heavy (c) or violent downpour (d).

The shape of the curves in Fig. 9a unambiguously indicates that the lowest resulting number of storm overflows (Z_t = 140) corresponds to the value a = 2.8 (scenario V). For the parameter value a = 1.0 (scenario I), the calculated number of storm overflows is Z_t = 152 and is larger by 12 than the number of storm overflows obtained in scenario V (a = 2.8). The largest resulting number of storm overflows (percentile 0.50), which equals Z_t = 162, corresponds to

828 the urbanisation dynamics in which the value of coefficient a is the lowest (a = 0.25; scenario
829 IV).
830 From the point of view of the number of storm overflows (t = 10 years), the concept of
831 urbanisation according to scenario V (a = 2.8) seems optimal. This results in the smallest
832 number of storm overflows (percentile 0.5). The considerable impact of the urbanisation of
833 urban catchment areas on the increase in the number of storm overflows and their volume in a
834 multiannual approach is confirmed in the paper by Shuster et al. (2005). These results remain
835 in compliance with the papers of Pennino et al. (2016). By analysing three catchment areas in
836 the Mid-Atlantic of the USA, the authors demonstrated the impacts of changes in the
837 imperviousness of the studied catchment areas (including solutions related to LID) on the
838 operations of storm overflows. The resulting relationships were also confirmed by the
839 calculations of Todeschini (2016), which were performed by means of a calibrated
840 hydrodynamic model using the example of a small catchment area in northern Italy. In that
841 case, the analysis of the impact of urbanisation dynamics in the catchment area in a
842 multiannual approach was performed within a limited scope, which, as demonstrated by the
843 present paper, is of major significance for the operation of an overflow (the number of
844 overflows). In relation to the spatial development plans of urban areas, the aspect analysed in
845 the paper is extremely important, as it provides the ability to plan the development and take
846 actions that allow the compensation of the disadvantageous impact of the catchment area
847 imperviousness on the quality of water in streams. This requires extending the proposed
848 methodology and taking into account both the volume and the pollution load in simulations.
849 The probability of the occurrence of a storm overflow in a period of t = 10 years caused by
850 moderate (p_m), heavy (p_h) or violent (p_s) downpours (Fig. 9b-d) was determined to increase
851 the level of detail of the abovementioned analyses. On the basis of the resulting curves, it was
852 concluded that, when a = 2.80 (scenario V), the resulting values of the probability of the

occurrence of a storm overflow caused by heavy and violent downpours were higher (Fig. 9c-d). Under the operating conditions of the network, this indicates an increase in the number of storm overflows, which also results in an increase of the pollution load introduced into the receiving waters. In terms of the probability of an storm overflow caused by moderate downpours, it was concluded that, among all considered scenarios (I-V), the lowest values of p_m were observed in scenarios III and V. A comparison of the calculation results (0.5 percentile) of the number of storm overflows determined by means of the developed mathematical model with the results of the continuous simulations (using the hydrodynamic model) resulted in their high similarity. This confirms the compliance of the relationships between the dynamics of changes in the imperviousness of the catchment area in a long-term approach, established through probabilistic and hydrodynamic models.

4.8. The impact of changes in rainfall dynamics and urbanisation on the multiannual number of overflows – sustainable development of the catchment area

The impact of changes in precipitation dynamics in consecutive years, as well as of the imperviousness of the catchment area (Imp), on the multiannual number of storm overflows is analysed below. Based on the parameters (μ, σ) determined in the theoretical distributions (tab. 2), simulations of rainfall series were performed by means of the I-C method with a LH modification. Considering the long period covered by the calculations and the fact that the variables used in the simulations are dependent, 2,500,000 samplings were performed for the 10-year rainfall series originating from the periods from 1990 to 1999 and from 1996 to 2005. During an intense increase in the imperviousness of the catchment area (Imp of 15%), a period of t_{cr} = 5 years was assumed. The reduction in the impervious area (t_{sust}) was also assumed to be 5 years. Tab. 3 presents values a and b for the modelled imperviousness scenarios, calculated using equation (17).

878

879 **Tab. 3.** List of the values of coefficients (a, b) in an empirical model describing Imp = *f*(t) in equation
880 (17).

Coefficient	Variant								
	I	II	III	IV	V	VI	VII	VIII	IX
a	1.0	0.4	2.4	1.0	1.0	0.4	0.4	2.4	2.4
b	1.0	0.4	2.4	0.4	2.4	1.0	2.4	1.0	0.4

881

882 The calculations assumed an initial impervious area of the catchment of $Imp_0 = 0.40$ and a
883 maximum impervious area of the catchment of $Imp_m = 0.55$; the impervious area of the
884 catchment after the period of $t_{cr} + t_{sust}$ was assumed to be $Imp_e = 0.47$. Simulations of the
885 operations of storm overflows were performed for the abovementioned assumptions in search
886 of an optimal scenario of changes in the imperviousness of the analysed catchment area. The
887 following were also determined on the same basis: the impact of changes in rainfall dynamics
888 in a multiannual approach and that of the imperviousness of the catchment area on the
889 multiannual number of storm overflows and the probability of the occurrence of a storm
890 overflow caused by moderate (p_m), heavy (p_h) and violent downpours (p_v). The calculation
891 results, i.e., the empirical distribution functions reflecting the probability of exceeding the 10-
892 year number of storm overflows and the probability of exceeding the occurrence probability
893 of a storm overflow resulting from moderate, heavy and violent downpours in scenarios I–IX
894 for the precipitation periods from 1990 to 1999 and from 1996 to 2005 are presented in
895 Appendixes F and G. A comparison between the respective values (0.5 percentile) of $Z_{t(0.5)}$
896 and $p_{m(0.5)}$ or $p_{h(0.5)}$ for the applied precipitation periods and imperviousness scenarios I-IX is
897 presented in Fig. 10. The yielded results are compared to the simulations that used the
898 hydrodynamic model. Due to the course of the empirical distribution function (Figs. 7d, 9b)
899 for violent downpours (compared to those for moderate and heavy downpours), the minimum

probability of exceeding the probability of a storm overflow (p_v) was presented for the scenarios covered by the calculations.

Based on the resulting curves, it was concluded that the number of storm overflows (percentile) derived from the probabilistic model is larger by maximum 2 storm overflows than that determined using the hydrodynamic model for the analysed scenarios (tab. 3). The resulting model confirms the high compliance of the calculation results obtained using the probabilistic model suggested in the manuscript in terms of a simultaneous simulation of the dynamics of changes in rainfall and the imperviousness of the catchment area.

Based on the performed analyses, it can be concluded that the smallest numbers of storm overflows derived from the theoretical distributions for the period from 1990 to 1999 were observed in scenarios III ($Z_{t(0.5)}$ = 133), and the largest value was observed in scenario II ($Z_{t(0.5)}$ = 140). For the period from 1996 to 2005 (similarly to the preceding period), the largest number of storm overflows was observed in scenario II and VI ($Z_{t(0.5)}$ = 148) and the smallest in scenario III ($Z_{t(0.5)}$ = 142). For linear increases in Imp in the period t_{cr} and rainfall in the period from 1990 to 1999, the smallest number of storm overflows ($Z_{t(0.5)}$ = 136) was observed in scenario V (b = 2.40) and the largest in scenario IV ($Z_{t(0.5)}$=139). The largest number of storm overflows in each of the consecutive computational scenarios, i.e., II, VI and VII (a = 0.40), as well as III, VIII and IX (a = 2.40), in both periods (1990-1999 and 1996-2005) were observed for b = 0.4 (Fig. 10a).

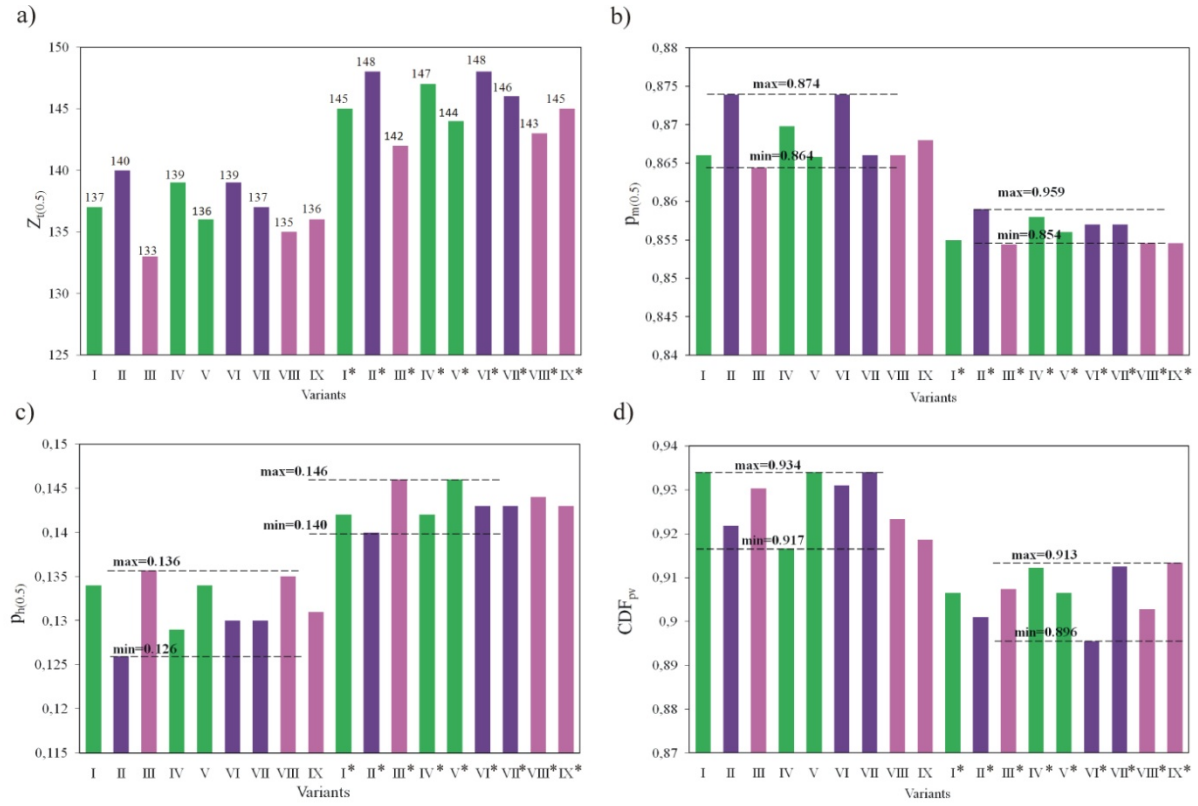

Fig. 10. Selected characteristics of storm overflows for imperviousness scenarios I – IX based on precipitation data in the periods from 1990 to 1999 and from 1996 to 2005 (marked with an asterisk): **a)** the number of storm overflows $Z_{t(0.5)}$ (per values); **b)** minimum probability of exceeding the probability of the occurrence of an storm overflow caused by violent downpours p_v (percentile 0.50); **c)** the probability of the occurrence of an storm overflow caused by moderate downpours $p_{m(0.5)}$ (percentile 0.50); and **d)** the probability of the occurrence of a storm overflow caused by heavy downpours $p_{h(0.5)}$ (percentile 0.50).

When assuming nonlinear dynamics of Imp = f(t) in period t_{cr} (a = 2.40 and b = 0.40), the resulting number of overflows or period t_{sust} (equation 14) was larger by 1 overflows than that of scenario VIII when b = 1.0. For scenario III, when a = b = 2.40, and for precipitation distributions for the period from 1990 to 1999, it was observed that the number of overflows Z_t = 133 was smaller by 4 overflows than that of scenario VII (a = 2.4 and b = 1.0) ($Z_{t(0.5)}$= 137). In scenario II and in the precipitation distribution for the period from 1990 to 1999, the number of overflows ($Z_{t(0.5)}$ =140) was larger by 4 overflows compared to that of scenario IX.

Figs. 10b-d demonstrate that a change in precipitation dynamics (moderate, heavy and violent downpours) had a significant impact on the probability of the occurrence of a storm overflow. The resulting values of $p_{m(0.5)}$ for the analysed scenarios, determined based on the theoretical distributions of precipitation in the period from 1990 to 1999, were lower than their counterparts from the 1996-2005 period. An identical relationship was observed with respect to the minimum probability of the occurrence of an storm overflow in a 10-year period for violent downpours (Fig. 10d). The values of the probability of an storm overflow caused by heavy downpours in the period from 1990 to 1999 were higher than their counterparts from the 1996-2005 period (Fig. 10c). In terms of the operation of a storm overflow, this means that it may be necessary to modify the position of the height of the overflow edges to limit the number of storm overflow events caused by precipitation with an average intensity of i = 10-50 mm·h^{-1}.

The interaction between the dynamics of changes in rainfall and the impervious area is of primary importance for the resulting number of storm overflows (10 years). For example, for the theoretical precipitation distributions in the period from 1990 to 1999 and for scenario II (tab. 3), the resulting number of storm overflows ($Z_{t(0.5)}$ = 140) was only 2 less than for the precipitation distributions for the period from 1996 to 2005 and scenario III. The dynamics of rainfall changes (caused by climate changes) presented using a long-term approach indicate an increase in the number of storm overflows. This is also confirmed by the simulation results obtained using hydrodynamic models (for a 30-year period) for urban catchment areas (Kleidorfer et al., 2014). The exclusion of the dynamics of changes in precipitation from the modelling process can result in the underestimation of the calculated number of storm overflows and, as a consequence, in the erroneous determination of the position of the edge of the overflow. The produced results unambiguously confirm the significant impacts of changes in precipitation dynamics and urbanisation on the functioning of storm overflows. This aspect

was analysed in detail in the paper by Wu et al. (2013). The authors presented the impacts of climate change and the impervious area of the catchment area on the runoff from the catchment to the receiving waters. The relationships demonstrated by these authors were confirmed by the work of other researchers who analysed catchment areas in the USA (Kirshen et al., 2014; Tavakol-Davani et al., 2016), Sweden (Semadeni-Davies et al., 2008) and Canada (Fortier and Mailhot, 2015; Jean et al., 2018).

The high compliance of the calculation results obtained using the probabilistic and hydrodynamic models indicates that the developed model constitutes a useful supporting tool when planning the directions of changes in the development of a catchment area (in a multiannual approach) in terms of reducing the number of storm overflows and therefore protecting water in streams. Due to the use of a simplified approach compared to that presented in previous papers (Kleidorfer et al., 2009; Thorndahl and Willems, 2008; Jean et al. 2019), the approach used in this paper can be applied to analyses in everyday engineering practice as an alternative to complicated hydrodynamic models requiring a large amount of data. Moreover, the developed rainfall generator allows modelling of the dynamics of its changes in a long-term approach, which, compared to the currently used models (Gironás et al., 2010; Arnell, 2011; Arnbjerg-Nielsen et al., 2013), constitutes a considerable simplification. The suggested computational methodology can be useful when constructing precipitation models by means of multidimensional density distributions used at the design stages of both the sewage system and the objects located above it.

5. Summary and conclusions

Currently, the modelling of objects (storm overflows, reservoirs, etc.) located in drainage networks, while taking into account the dynamics of precipitation and urbanisation in short- and long-term approaches, constitutes a topical issue. The calculations performed in this paper

indicated that a logistic regression model can be used for predicting the operation of a storm overflow during a precipitation event. The action of an overflow can be modelled based on the average rainfall intensity and the impervious area of the catchment; this constitutes a simplification compared to the work of other authors. The logistic regression model has been verified for different catchment area imperviousness values by means of simulations using a hydrodynamic model. The produced calculation results confirmed that the approach used in this paper has a universal nature and can be used for catchment areas with diverse physical-geographical characteristics.

The paper proves that modifications to the forms of empirical models used for predicting the parameters of statistical distributions depending on the time, as included in the Monte Carlo method, allows the modelling of changes in rainfall dynamics, which translates into the modelling of the number of storm overflows. The performed simulations demonstrated that the methodology suggested in the paper could be applied to simulations of short- and long-term rainfall series considering the changes in their dynamics. The suggested computational methodology has a universal nature and enables its implementation when modelling the operations of sewage networks and objects located above them while considering changes in precipitation dynamics.

It was also concluded that the proposed probabilistic model allows the assessment of the impacts of changes in land development and the dynamics of changes in rainfall intensity in consecutive years on the occurrence of an overflow in a precipitation event and in a multiannual aspect. The resulting model allows optimisation of the selection of the concept of sustainable development for a catchment area, considering, on the one hand, changes in rainfall dynamics and, on the other hand, the impervious area of the catchment, which so far has not been studied in detail by other authors. The results produced in this manner confirmed that the proposed model constitutes a useful tool for analysing the operation of a storm

overflow (and for predicting the occurrence of a storm overflow) and provides the ability to test various scenarios involving the development of catchment areas, even at their conceptual stages.

The performed simulations proved that the dynamics of land development have strong impacts on the number of overflows and their changes in the following years. The smallest number of overflows in a multiannual aspect was achieved for scenarios in which the urbanisation process in the initial period covered by the simulations proceeded slowly. In contrast, in a scenario in which significant changes take place during the initial period of urbanisation, the simulation resulted in the largest number of storm overflows.

The yielded results confirmed the impacts of changes in precipitation dynamics in consecutive years on the probability of the occurrence of a storm overflow, which decreased for moderate precipitation. In contrast, a considerable increase was recorded in the case of storm overflows caused by heavy and violent downpours. Therefore, there is a need for further analyses intended to expand the model described in the present paper by the consideration of other variables (e.g., the height of the storm overflow), which will allow a dynamic modification of the operating conditions of the studied storm overflow in a multiannual time interval.

Appendix

Appendix A. Change of the impervious area of the catchment in the years 2009-2019.

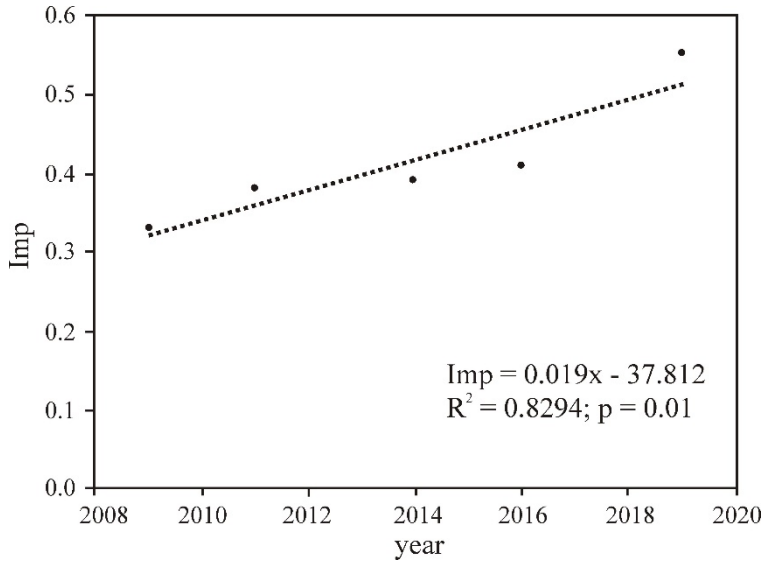

Appendix B. Results of computations of μ and σ of polynomials.

Degree of a polynomial	μ			σ		
	RMSE	AIC	R^2	RMSE	AIC	R^2
1	0.012187	-21.1118	0.8886	0.008	-28.37	0.5374
2	0.001172	-22.5467	0.9356	0.005	-33.66	0.8574
3	0.010740	-19.1734	0.9498	0.008	-23.16	0.8691

Appendix C. The values of the Spearman's correlation coefficients between the values of average rainfall intensity in precipitation events (i) in the consecutive years of a multiannual time interval.

	1961	1962	1963	1964	1965	1966	1967	1968	1969	1970	1971	1972	1973	1974	1975	1976
1961	1.00	0.82	0.84	0.76	0.70	0.63	0.51	0.41	0.30	0.21	-0.03	-0.11	-0.20	-0.26	-0.34	-0.41
1962		1.00	0.82	0.81	0.78	0.71	0.59	0.49	0.37	0.29	0.04	-0.05	-0.14	-0.19	-0.28	-0.34
1963			1.00	0.82	0.82	0.79	0.67	0.57	0.45	0.37	0.11	0.03	-0.06	-0.12	-0.21	-0.27
1964				1.00	0.84	0.81	0.75	0.64	0.53	0.45	0.18	0.10	0.00	-0.05	-0.14	-0.20
1965					1.00	0.83	0.81	0.71	0.59	0.51	0.23	0.15	0.05	0.00	-0.09	-0.16
1966						1.00	0.78	0.78	0.67	0.58	0.30	0.22	0.12	0.06	-0.02	-0.09
1967							1.00	0.80	0.79	0.70	0.41	0.32	0.23	0.17	0.08	0.02
1968								1.00	0.79	0.80	0.51	0.42	0.33	0.27	0.18	0.12
1969									1.00	0.81	0.61	0.52	0.43	0.37	0.28	0.21
1970										1.00	0.69	0.60	0.50	0.44	0.35	0.29
1971											1.00	0.82	0.82	0.75	0.65	0.57
1972												1.00	0.80	0.81	0.73	0.66
1973													1.00	0.82	0.80	0.76
1974														1.00	0.81	0.81
1975															1.00	0.81
1976																1.00

Appendix D. The Iman-Conover (IC) method.

The following conditions must be fulfilled to confirm the correctness of the results produced by the Iman-Conover method:

- in data resulting from simulations and measurements, the average value and standard deviations for the investigated dependent variables in samples cannot differ by more than 5%,
- the theoretical distributions of dependent variables resulting from the simulations must comply with those resulting from the measurements; to fulfil this condition, it is recommended to perform the Kolmogorov-Smirnov test, and
- the value of the Spearman's correlation coefficient (R) between dependent variables (x_i) corresponding to the data from simulations cannot differ by more than 5% from the R value derived from the empirical data.

When the abovementioned conditions are fulfilled, the results of the calculations performed by means of the IC method may be deemed correct. In contrast, when one of the abovementioned conditions is not fulfilled, it is necessary to increase the sample size.

1053 **Appendix E**. Results of the calculations of test probability values *p* for selected statistical distributions

1054 (Gumbel, Weibull, Frechet, Gamma).

Period	p-test							
	Gumbel		Weibull		Frechet		Gamma	
	K-S	χ^2	K-S	χ^2	K-S	χ^2	K-S	χ^2
1961-1990	0.0048	0.0030	0.0216	0.0210	0.0074	0.0068	0.0185	0.0141
1962-1991	0.0050	0.0021	0.0224	0.0212	0.0065	0.0064	0.0170	0.0123
1963-1992	0.0048	0.0042	0.0234	0.0273	0.0066	0.0053	0.0177	0.0115
1964-1993	0.0059	0.0023	0.0236	0.0214	0.0056	0.0051	0.0195	0.0128
1965-1994	0.0050	0.0034	0.0238	0.0236	0.0055	0.0044	0.0238	0.0211
1966-1995	0.0057	0.0035	0.0222	0.0222	0.0047	0.0042	0.0202	0.0149
1967-1996	0.0041	0.0023	0.0230	0.0243	0.0038	0.0028	0.0194	0.0111
1968-1997	0.0043	0.0022	0.0234	0.0247	0.0037	0.0033	0.0201	0.0148
1969-1998	0.0042	0.0031	0.0234	0.0227	0.0037	0.0031	0.0185	0.0110
1970-1999	0.0029	0.0025	0.0225	0.0221	0.0047	0.0032	0.0177	0.0138
1971-2000	0.0041	0.0027	0.0226	0.0224	0.0038	0.0029	0.0141	0.0129
1972-2001	0.0031	0.0023	0.0241	0.0213	0.0037	0.0028	0.0184	0.0168
1973-2002	0.0047	0.0041	0.0208	0.0249	0.0037	0.0031	0.0220	0.0177
1974-2003	0.0050	0.0032	0.0257	0.0258	0.0046	0.0039	0.0255	0.0211
1975-2004	0.0040	0.0023	0.0265	0.0257	0.0038	0.0042	0.0232	0.0209
1976-2005	0.0058	0.0031	0.0257	0.0253	0.0028	0.0032	0.0197	0.0168

1055

Appendix F. Multiannual (t = 10 years) characteristics of overflows for imperviousness scenarios I, IV and V, based on the theoretical distributions of precipitation in the periods from 1990 to 1999 and from 1996 to 2005: **a)** the number of overflows; **b-d)** the probability of the occurrence of a overflow caused by a moderate (b), heavy (c) or violent (d) downpour.

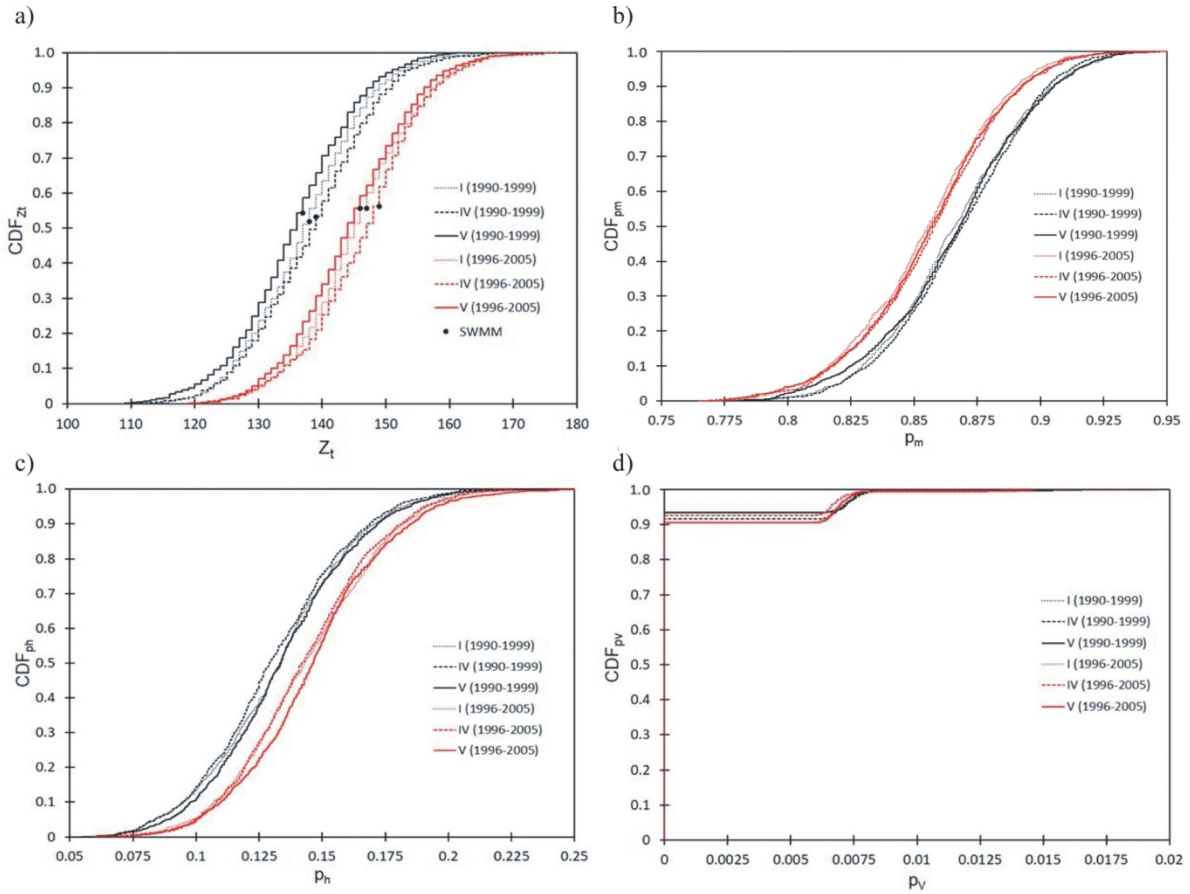

1062 **Appendix G.** Multiannual (t = 10 years) characteristics of overflows for imperviousness scenarios III,
1063 VIII and IX, based on the theoretical distributions of precipitation in the periods from 1990 to 1999
1064 and from 1996 to 2005: **a)** the number of overflows; **b-d)** the probability of the occurrence of a
1065 overflow caused by a moderate (b), heavy (c) or violent (d) downpour.

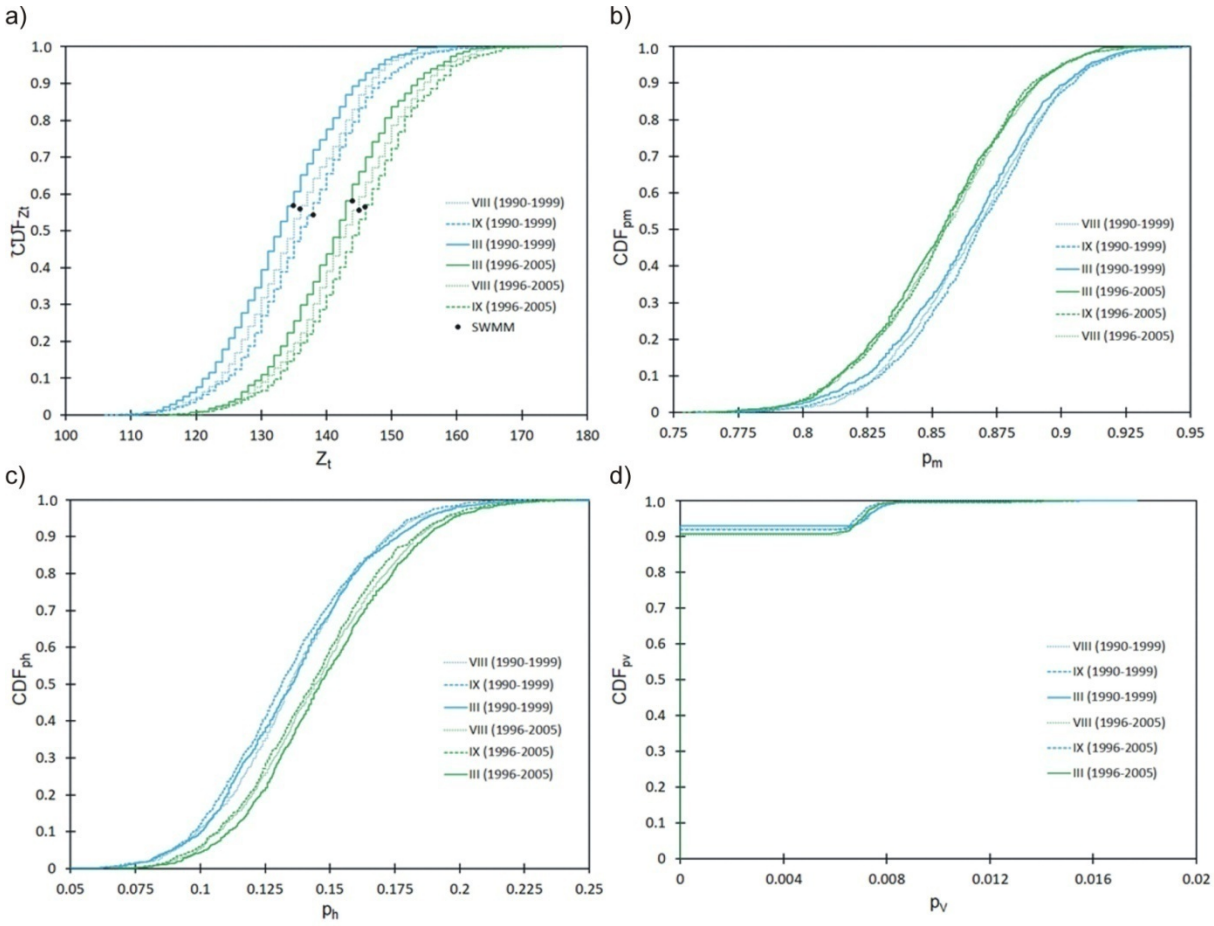

1066

1067

1068 **Appendix H.** Multiannual (t = 10 years) characteristics of overflows for imperviousness scenarios II,
1069 VI and VII, based on the theoretical distributions of precipitation in the periods from 1990 to 1999 and
1070 from 1996 to 2005: **a)** the number of overflows; **b-d)** the probability of the occurrence of a overflow
1071 caused by a moderate (b), heavy (c) or violent (d) downpour.

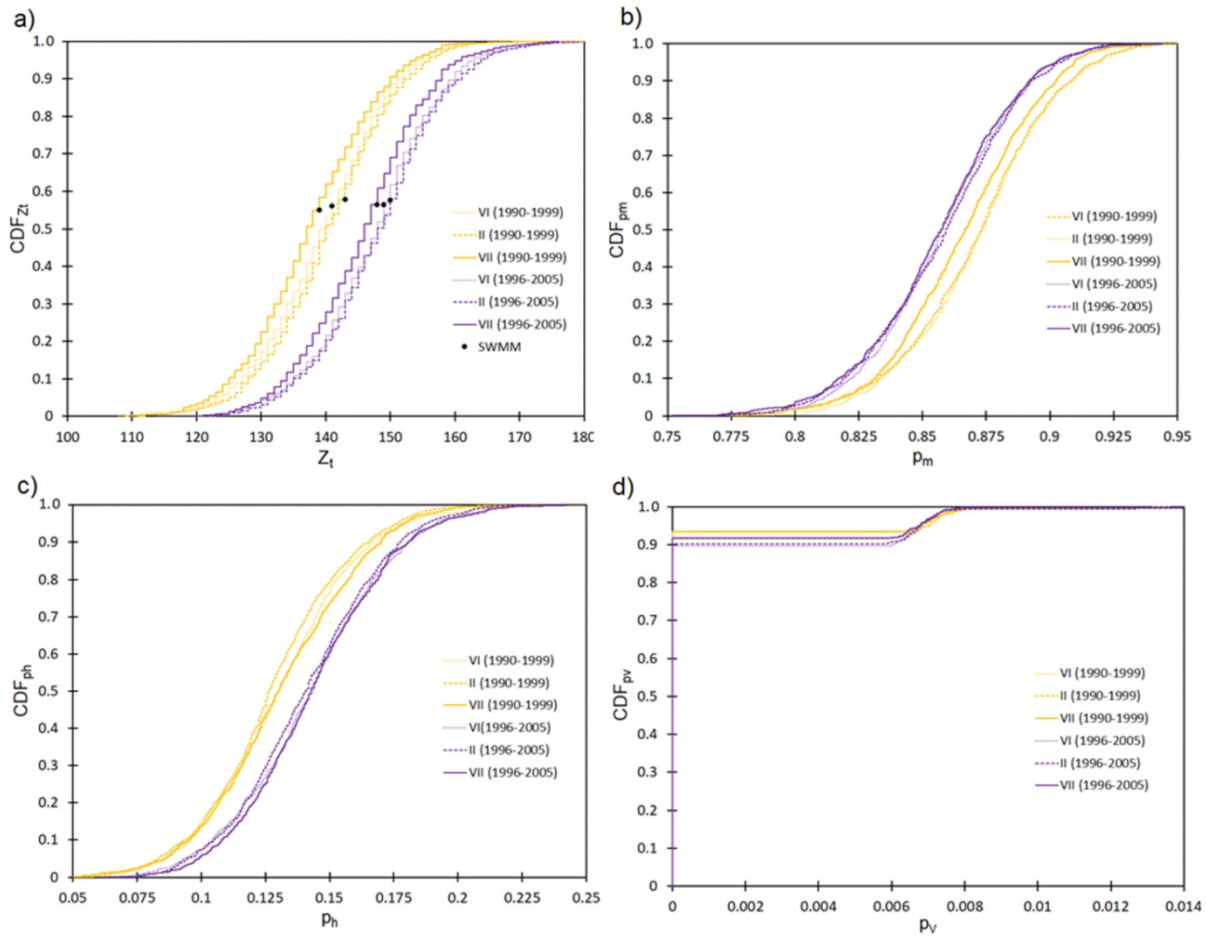

1072

1073

References

Abdellatif, M., Atherton W., Alkhaddar, R.M., Osman, Y.Z., 2015. Quantitative assessment of sewer overflow performance with climate change in northwest England. Hydrol. Sci. J. 60(4), 636–650. https://doi.org/10.1080/02626667.2014.912755.

Adams, B.J., Papa, F., 2000. Urban Stormwater Management Planning with Analytical Probabilistic Models. John Wiley & Sons, Chichester, England.

Arnbjerg-Nielsen, K., Willems, P., Olsson, J., Beecham, S., Pathirana, A., Bülow Gregersen, I., Madsen, H., Nguyen, V.T.V., 2013. Impacts of climate change on rainfall extremes and urban drainage systems: A review. Water Sci. Technol. 68(1), 16–28. https://doi.org/10.2166/wst.2013.251.

Arnell, N.W., 2011. Uncertainty in the relationship between climate forcing and hydrological response in catchments. Hydrol. Earth Syst. Sci. 15, 897–912. https://doi.org/10.5194/hess-15-897-2011.

Bates, B.C., Kundzewicz, Z.W., Wu, S., Palutikof, J.P., 2008. Climate Change and Water. Technical Paper of the Intergovernmental Panel on Climate Change. IPCC Secretariat, Geneva, Switzerland.

Bendel, D., Beck, F., Dittmer, U., 2013. Modeling climate change impacts on combined sewer overflow using synthetic precipitation time series. Water Sci. Technol. 68(1), 160–166. https://doi.org/10.2166/wst.2013.236.

Bixio, D., Parmentier, G., Rousseau, D., Verdonck, F., Meirlaen, J., Vanrolleghem, P.A., Thoeye, C., 2002. A quantitative risk analysis tool for design/simulation of wastewater treatment plants. Water Sci. Technol. 46(4–5), 301–307. https://doi.org/10.2166/wst.2002.0611.

1097 Boyle, J.S., 1998. Evaluation of the annual cycle of precipitation over the United States in
1098 GCMs: AMIP simulations. J. Clim. 11(5), 1041–1055. https://doi.org/10.1175/1520-
1099 0442.
1100 D'Agostino, R.B., 2017. Goodness-of-Fit-Techniques. Routledge, Abingdon, UK.
1101 De Paola, F., Ranucci, A., 2012. Analysis of spatial variability for stormwater capture tank
1102 assessment. Irrig. Drain. 61, 682–690. https://doi.org/10.1002/ird.1675.
1103 DWA-A 118E, 2006. Hydraulic Dimensioning and Verification of Drain and Sewer Systems.
1104 DWA German Association for Water, Wastewater and Waste, Hennef, Germany.
1105 DWA-M 180E, 2005. Framework for planning of real time control of sewer networks, DWA
1106 German Association for Water, Wastewater and Waste, Hennef, Germany.
1107 Elliott, A.H., Trowsdale, S.A., 2007. A review of models for low impact urban stormwater
1108 drainage. Environ. Modell. Softw. 22(3), 394–405. https://doi.org/10.1016/
1109 j.envsoft.2005.12.005.
1110 Espino, D.J., Sillanpää, N., Doménech, I.A., Hernandez J.R., 2018. Flood Risk Assessment in
1111 Urban Catchments Using Multiple Regression Analysis. J. Water Resour. Plann. Manage.
1112 144(2), 4017085. https://doi.org/10.1061/(ASCE)WR.1943-5452.0000874.
1113 Forrester, A.I.J., Keane, A.J., 2017. Characterization of Geometric Uncertainty in Gas
1114 Turbine Engine Components using CMM Data. In: 12th World Congress on Structural
1115 and Multidisciplinary Optimization, 5-9 June 2017, Braunschweig, Germany.
1116 Fortier, C. Mailhot, A., 2015. Climate Change Impact on Combined Sewer Overflows. J.
1117 Water Resour. Plann. Manage. 141(5), 1–7. https://doi.org/10.1061/(ASCE)WR.1943-
1118 5452.0000468.
1119 Fu, G., Butler, D., Khu, S.T., Sun, S., 2014. Imprecise probabilistic evaluation of sewer
1120 flooding in urban drainage systems using random set theory. Water Resour. Res. 47(2),
1121 1–13. https://doi.org/10.1029/2009WR008944.

1122 Fu, G., Kapelan, Z., 2013. Flood analysis of urban drainage systems: probabilistic dependence
1123 structure of rainfall characteristics and fuzzy model parameters. J. Hydroinform. 15(3),
1124 687–699. https://doi.org/10.2166/hydro.2012.160.
1125 Ganguli, P., Coulibaly, P., 2019. Assessment of future changes in intensity-duration-
1126 frequency curves for Southern Ontario using North American (NA)-CORDEX models
1127 with nonstationary methods. J. Hydrol. Reg. Stud. 22, 1–22. https://doi.org/10.1016/
1128 j.ejrh.2018.12.007.
1129 Gironás, J., Roesner, L.A., Rossman, L.A., Davis, J., 2010. A new applications manual for the
1130 Storm Water Management Model (SWMM). Environ. Modell. Softw. 25(6), 813–814.
1131 https://doi.org/10.1016/j.envsoft.2009.11.009.
1132 Grum, M., Aalderink, R.H., 1999. Uncertainty in return period analysis of combined sewer
1133 overflow effects using embedded Monte Carlo simulations. Water Sci. Technol. 39(4),
1134 233–240. https://doi.org/10.1016/S0273-1223(99)00063-3.
1135 Guo, J., Urbonas, B., 2002. Runoff Capture and Delivery Curves for StormWater Quality
1136 Control Designs. J. Water Resour. Plan. Manag. 128(3), 208–215.
1137 https://doi.org/10.1061/(ASCE)0733-9496(2002)128:3(208).
1138 Huong, H.T.L., Pathirana, A., 2013. Urbanization and climate change impacts on future urban
1139 flooding in Can Tho city, Vietnam. Hydrol. Earth Syst. Sci. 17, 379–394.
1140 https://doi.org/10.5194/hess-17-379-2013.
1141 Iman, R.L., Conover, W.J., 1982. A distribution-free approach to inducing rank correlation
1142 among imput variables. Commun. Stat. Simulat. 11, 311–334. https://doi.org//
1143 10.1080/03610918208812265.
1144 Jean, M.È., Duchesne, S., Pelletier, G., Pleau, M., 2018. Selection of rainfall information as
1145 input data for the design of combined sewer overflow solutions. J. Hydrol. 565, 559–569.
1146 https://doi.org/10.1016/j.jhydrol.2018.08.064.

1147 Jean, M.È., Duchesne, S., Pelletier, G., Pleau, M., 2019. Conceptual Framework for
1148 Integrating Real-Time Control and Source Control Solutions for CSO Frequency Control.
1149 In: Mannina, G. (Ed.), New Trends in Urban Drainage Modelling. UDM 2018. Green
1150 Energy and Technology, Springer, Cham. 614–620. https://doi.org/10.1007/978-3-319-
1151 99867-1_106.
1152 Kaźmierczak, K., Kotowski A., 2015. The suitability assessment of a generalized exponential
1153 distribution for the description of maximum precipitation amounts. J. Hydrol. 525, 345–
1154 351. https://doi.org/ 10.1016/j.jhydrol.2015.03.063.
1155 Khudhair, B., Khalid, G., Jbbar, R., 2019. Condition prediction models of deteriorated trunk
1156 sewer using multinomial logistic regression and artificial neural network. Int. J. Civ. Eng.
1157 10(1), 93–104.
1158 Kirshen, P., Caputo, L., Vogel, R.M., Mathisen, P., Rosner, A., Renaud T., 2014. Adapting
1159 Urban Infrastructure to Climate Change: A Drainage Case Study. J. Water Res. Plann.
1160 Manage. 141(4), 04014064. https://doi.org/10.1061/(ASCE)WR.1943-5452.0000443.
1161 Kleidorfer, M., Möderl, M., Sitzenfrei, R., Urich, C., Rauch, W., 2009. A case independent
1162 approach on the impact of climate change effects on combined sewer system
1163 performance. Water Sci. Technol. 60(6), 1555–1564.
1164 https://doi.org/10.2166/wst.2009.520.
1165 Kleidorfer, M., Mikovits, C., Jasper-Tönnies, A., Huttenlau, M., Einfalt, T., Rauch, W., 2014.
1166 Impact of a changing environment on drainage system performance. Procedia Eng. 70,
1167 943–950. https://doi.org/10.1016/j.proeng.2014.02.105.
1168 Kupczyk, E., Suligowski, R., 1997. Statistical description of the rainfall structure as the input
1169 to hydrological models. In: Soczyńska, U. (Ed.), Prediction of the design storms and
1170 floods. University of Warsaw Publisher, Warsaw, pp. 191–212.

1171 Liu, Y., Engel, B.A., Flanagan, D.C., Gitau, M.W., Millan S.K.M., Chaubey, I., 2017. A
1172 review on effectiveness of best management practices in improving hydrology and water
1173 quality: Needs and opportunities. Sci Total Environ. 601–602, 580–593.
1174 https://doi.org/10.1016/j.scitotenv.2017.05.212.
1175 Maronati,G., Petrovic, B., 2019. Estimating cost uncertainties in nuclear power plant
1176 construction through Monte Carlo sampled correlated random variables. Prog. Nucl.
1177 Energy 111, 211-222. https://doi.org/10.1016/j.pnucene.2018.11.011.
1178 McGrane, S.J., 2016. Impacts of urbanisation on hydrological and water quality dynamics,
1179 and urban water management: a review. Hydrol. Sci. J. 61(13), 2295–2311.
1180 https://doi.org/10.1080/02626667.2015.1128084
1181 Pennino, M.J., McDonald, R.I., Jaffe, P.R., 2016. Watershed-scale impacts of stormwater
1182 green infrastructure on hydrology, nutrient fluxes, and combined sewer overflows in the
1183 mid-Atlantic region. Sci. Total Environ. 565, 1044–1053. https://doi.org/10.1016/
1184 j.scitotenv.2016.05.101.
1185 Salman, B., Salem, O., 2012. Modeling failure of wastewater collection lines using various
1186 section-level regression models. J. Infrastruct. Syst. 18(2), 146–154.
1187 https://doi.org/10.1061/(ASCE)IS.1943-555X.0000075.
1188 Sarhadi, A., Soulis, E.D., 2017. Time-varying extreme rainfall intensity-duration-frequency
1189 curves in a changing climate. Geophys. Res. Lett. 44, 2454–2463.
1190 https://doi.org/10.1002/2016GL072201.
1191 Savapandit, R.R., Gogoi. B., 2015. Bootstrap and Other Tests for Goodness of Fit. Sci. Math.
1192 Jpn. 78(4), 99-110. https://doi.org/10.32219/isms.78.4-Special_99.
1193 Semadeni-Davies, A., Hernebring, C., Svensson, G., Gustafsson, L-G., 2008. The impacts of
1194 climate change and urbanisation on drainage in Helsingborg, Sweden: Combined sewer
1195 system. J. Hydrol. 350, 100–113. https://doi.org/10.1016/j.jhydrol.2007.05.028.

1196 Sharma, D., Das Gupta, A., Babel, M.S., 2007. Spatial disaggregation of bias-corrected GCM
1197 precipitation for improved hydrologic simulation: Ping River Basin, Thailand. Hydrol.
1198 Earth Syst. Sci. 11, 1373–1390. https://doi.org/10.5194/hess-11-1373-2007.
1199 Shuster, W.D., Bonta, J., Thurston, H., Warnemuende, E., Smith, D.R., 2005. Impacts of
1200 Impervious Surface on Watershed Hydrology. A review. Urban Water J. 2(4), 263–275.
1201 https://doi.org/10.1080/15730620500386529.
1202 Stephens, M.A., 1974. EDF Statistics for Goodness of Fit and Some Comparisons. J. Am.
1203 Stat. Assoc. 69(347), 730–737. https://doi.org/10.2307/2286009.
1204 Suligowski, R., 2004. Temporal and spatial structure of rainfall in Poland: regionalization
1205 attempt. PhD thesis, Warsaw University.
1206 Sumner, G., 1988. Precipitation: process and analysis. John Wiley & Sons, Chichester,
1207 England.
1208 Szeląg, B., Cienciała, A., Sobura, S., Studziński, J., García, J.T., 2019. Urbanization and
1209 Management of the Catchment Retention in the Aspect of Operation of Storm Overflow:
1210 A Probabilistic Approach. Sustainability 11, 3651. https://doi.org/10.3390/su11133651.
1211 Szeląg, B., Kiczko, A., Dąbek, L., 2016. Sensitivity and uncertainty analysis of hydrodynamic
1212 model (SWMM) for storm water runoff forecating in an urban basin – a case study.
1213 Ochrona Środowiska 38(3), 15–22.
1214 Szeląg, B., Kiczko, A., Studziński, J., Dąbek, L., 2018. Hydrodynamic and probabilistic
1215 modelling of storm overflow discharges. J. Hydroinform. 20(5), 1100–1110.
1216 https://doi.org/10.2166/hydro.2018.005.
1217 Szeląg, B., Suligowski, R., Studziński, J., De Paola, F., 2020. Application of logistic
.218 regression to simulate the influence of rainfall genesis on storm overflow operations: a
.219 probabilistic approach. Hydrol. Earth Syst. Sci. 24, 595–614.
.220 https://doi.org/10.5194/hess-24-595-2020.

1221 Talebizadeh M., Belia E., Vanrolleghem P.A., 2014. Probability-based design of wastewater
1222 treatment plants. In: Ames, D.P., Quinn, N.W.T., Rizzoli, A.E. (Eds.), Proceedings of the
1223 7th International Congress on Environmental Modelling and Software, 15–19 June 2014,
1224 San Diego, CA, USA.
1225 Tavakol-Davani, H., Goharian, E., Hansen, C.H., Tavakol-Davani, H., Apul, D., Burian, S.J.,
1226 2016. How does climate change affect combined sewer overflow in a system benefiting
1227 from stormwater harvesting systems? Sustain. Cities Soc. 77, 430–438.
1228 http://dx.doi.org/10.1016/j.scs.2016.07.003.
1229 Todeschini, S., 2016. Hydrologic and Environmental Impacts of Imperviousness in an
1230 Industrial Catchment of Northern Italy. J. Hydrol. Eng. 21(7), 1943–1955. https://doi.org/
1231 10.1061/(ASCE)HE.1943-5584.0001348.
1232 Thorndahl, S., Willems, P., 2008. Probabilistic modelling of overflow, surcharge and flooding
1233 in urban drainage using the first order reliability method and parameterization of local
1234 rain series. Water Res. 42(1–2), 455–466. https://doi.org/10.1016/j.watres.2007.07.038.
1235 Wang, C., Zeng, B., Shao. J., 2011. Application of Bootstrap Method in Kolmogorov-
1236 Smirnov Test. In: International Conference on Quality, Reliability, Risk, Maintenance,
1237 and Safety Engineering, 17th-19th June 2011, Xi'an, China. pp. 287–291.
1238 https://doi.org/10.1109/ICQR2MSE.2011.5976614.
1239 World Meteorological Organization, 2012. Guide to Meteorological Instruments and Methods
1240 of Observation. WMO No. 8, Geneva, Switzerland.
1241 Wu, J.Y., Thompson, J.R., Kolka, R.K., Franz, K.J., Stewart, T.W. 2013. Using the Storm
1242 Water Management Model to predict urban headwater stream hydrological response to
1243 climate and land cover change. Hydrol. Earth Syst. Sci. 17, 4743–4758.
1244 https://doi.org/10.5194/hess-17-4743-2013.

1245 Zhang, K., Fong, T., Chui, M., 2018. A comprehensive review of spatial allocation of LID-
1246 BMP-GI practices: Strategies and optimization tools. Sci. Total Environ. 621, 915–929.
1247 https://doi.org/10.1016/j.scitotenv.2017.11.281.